© 2014. Published by The Company of Biologists Ltd | Journal of Cell Science (2014) 127, 977–993 doi:10.1242/jcs.136598

RESEARCH ARTICLE

# Cytosolic phospholipase $A_2\varepsilon$ drives recycling through the clathrin-independent endocytic route

**Mariagrazia Capestrano[1], Stefania Mariggio[2], Giuseppe Perinetti[1], Anastasia V. Egorova[3], Simona Iacobacci[3], Michele Santoro[3], Alessio Di Pentima[1], Cristiano Iurisci[1], Mikhail V. Egorov[3], Giuseppe Di Tullio[1], Roberto Buccione[1], Alberto Luini[2,3] and Roman S. Polishchuk[3,*]**

## ABSTRACT

Previous studies have demonstrated that membrane tubule-mediated transport events in biosynthetic and endocytic routes require phospholipase $A_2$ ($PLA_2$) activity. Here, we show that cytosolic phospholipase $A_2\varepsilon$ ($cPLA_2\varepsilon$, also known as PLA2G4E) is targeted to the membrane compartments of the clathrin-independent endocytic route through a C-terminal stretch of positively charged amino acids, which allows the enzyme to interact with phosphoinositide lipids [especially $PI(4,5)P_2$] that are enriched in clathrin-independent endosomes. Ablation of $cPLA_2\varepsilon$ suppressed the formation of tubular elements that carry internalized clathrin-independent cargoes, such as MHC-I, CD147 and CD55, back to the cell surface and, therefore, caused their intracellular retention. The ability of $cPLA_2\varepsilon$ to support recycling through tubule formation relies on the catalytic activity of the enzyme, because the inactive $cPLA_2\varepsilon^{S420A}$ mutant was not able to recover either tubule growth or transport from clathrin-independent endosomes. Taken together, our findings indicate that $cPLA_2\varepsilon$ is a new important regulator of trafficking processes within the clathrin-independent endocytic and recycling route. The affinity of $cPLA_2\varepsilon$ for this pathway supports a new hypothesis that different $PLA_2$ enzymes use selective targeting mechanisms to regulate tubule formation locally during specific trafficking steps in the secretory and/or endocytic systems.

**KEY WORDS: MHC-I trafficking, Clathrin-independent endocytosis, Membrane curvature, Phospholipase A2, Recycling tubules**

## INTRODUCTION

To keep the identity and composition of the surface domains and the membrane intracellular organelles, eukaryotic cells develop transport mechanisms that allow precise delivery of the protein and lipid molecules to the specific target compartments. The membrane trafficking of newly synthesized or endocytosed molecules is executed by the membrane-bound organelles called transport carriers that emerge from a donor compartment, move through the cytosol and fuse with an acceptor compartment (Luini et al., 2005; Polishchuk et al., 2009).

[1]Consorzio Mario Negri Sud, 66030 Santa Maria Imbaro (Chieti), Italy. [2]Institute of Protein Biochemistry National Research Council, Via Pietro Castellino 111, 80131 Naples, Italy. [3]Telethon Institute of Genetics and Medicine (TIGEM), Via P. Castellino 111, 80131 Naples, Italy.

*Author for correspondence (polish@tigem.it)

**Received 14 June 2013; Accepted 9 December 2013**

Budding of transport carriers requires bending of the donor membrane, which can be achieved through several molecular mechanisms. Interaction with protein coat polymers, BAR domains, amphipathic wedges and the components of cytoskeleton machineries have been reported to deform the plain membrane domains into highly curved buds (Graham and Kozlov, 2010; McMahon and Gallop, 2005). However, induction of membrane curvature for biogenesis of transport carriers could be triggered through a local transfer and/or modification of lipids molecules, which are executed by either lipid-transfer proteins or lipid-modifying enzymes, respectively (Graham and Kozlov, 2010; Sprong et al., 2001).

Among the lipid-modifying enzymes, cytosolic phospholipase $A_2$ ($PLA_2$) has been hypothesized to support the budding of tubular transport carriers because these enzymes hydrolyze cylinder-shaped phospholipids into wedge-like lysophospholipids (Bechler et al., 2012; Ha et al., 2012). This change in lipid geometry favors the generation of positive membrane curvature, which is required for budding of tubular carriers (Bechler et al., 2012; Ha et al., 2012; San Pietro et al., 2009). Although $PLA_2$ activity is required for the transport of both newly synthesized and endocytosed proteins, which $PLA_2$ enzymes operate in regulation of specific traffic events in either biosynthetic or endocytic routes remains poorly understood. Over the past few years, two cytosolic $PLA_2$ enzymes have been reported to regulate the formation of tubular elements that operate in different transport steps. Cytosolic $Ca^{2+}$-dependent $PLA_2\alpha$ ($cPLA_2\alpha$, also known as PLA2G4A) operates in intra-Golgi trafficking (San Pietro et al., 2009), whereas cytoplasmic $PLA_2$ enzyme complex platelet-activating factor acetylhydrolase (PAFAH) Ib regulates protein export from the Golgi at the TGN level (Bechler et al., 2010) and the distribution and function of endosomes (Bechler et al., 2011). Therefore, it is likely that different $PLA_2$ enzymes operate in various specific tubule-mediated transport steps. As a consequence, each individual compartment of either the secretory or endocytic system must acquire its own $PLA_2$ enzyme to generate tubular transport carriers when needed.

In the endocytic system, a wide range of transport events rely on tubular membrane structures (Bonifacino and Rojas, 2006; Cullen, 2008; Polishchuk et al., 2009) and therefore might require specific $PLA_2$ enzymes. Indeed, $PLA_2$ activity has been demonstrated to support endosome tubulation and recycling of endocytosed material back to the cell surface (Bechler et al., 2011; de Figueiredo et al., 2001; Doody et al., 2009). Moreover, identification of several novel $PLA_2$ isoforms revealed their association with the endo/lysosomal system (Ghosh et al., 2006a; Ohto et al., 2005). However, the role of these recently identified $PLA_2$ enzymes in transport through well-defined endocytic and recycling pathways remains elusive.



Journal of Cell Science

Journal of Cell Science (2014) 127, 977–993 doi:10.1242/jcs.136598

We show here that cPLA$_2$ε binds to the membranes of the clathrin-independent transport pathway that is involved in the uptake and recycling of specific cargoes, such as major histocompatibility complex class I (MHC-I) proteins. This association relies on the C-terminal stretch of positively charged amino acids that binds to several phosphoinositide phosphate (PIP) lipids. Silencing of cPLA$_2$ε significantly inhibits the formation of tubular elements involved in the recycling of internalized MHC-I and therefore induces intracellular accumulation of MHC-I. The capacity of cPLA$_2$ε to support recycling of MHC-I through tubule formation requires catalytic activity of the enzyme because the inactive cPLA$_2$ε mutant does not rescue MHC-I transport. Taken together, our findings indicate that cPLA$_2$ε is an important player in transport events within the clathrin-independent endocytic or recycling route and support the hypothesis that specific targeting mechanisms of PLA$_2$ enzymes to different intracellular compartments could be needed to regulate tubule formation in diverse segments of secretory and endocytic pathways.

## RESULTS

PLA$_2$ activity has been reported to support the formation of membranous tubular elements operating in the endocytic system (de Figueiredo et al., 2001; Doody et al., 2009). We thus sought to identify the PLA$_2$ isoform(s) involved in the regulation of transport events within the endocytic pathway. The superfamily of PLA$_2$ enzymes consists of 16 groups (Dennis et al., 2011) comprising secretory and cytosolic enzymes, with the latter divided into $Ca^{2+}$-sensitive (cPLA$_2$s, or group IV PLA$_2$s) and $Ca^{2+}$-insensitive (group VI, VII and VIII PLA$_2$) isoforms (Schaloske and Dennis, 2006). Among those that are $Ca^{2+}$ sensitive, cPLA$_2$ε has been reported to associate with the membranes of the endo/lysosomal system (Ohto et al., 2005). This affinity for the membranes of endocytic compartments prompted us to examine whether cPLA$_2$ε might itself be involved in tubule formation and trafficking through the specific endocytic route.

### cPLA$_2$ε resides on the membranes of the clathrin-independent endocytic/recycling route

Given that the association of cPLA$_2$ε with any specific endocytic/recycling pathway has not yet been investigated in detail, we analyzed the intracellular distribution of the cPLA$_2$ε using a battery of the markers that label different endocytic compartments and pathways. HeLa cells transfected with cPLA$_2$ε–GFP exhibited a clear fluorescent signal at the plasma membrane as well as along a number of intracellular tubular (Fig. 1, arrows) and vacuolar structures (Fig. 1, arrowheads). Such tubular elements decorated by cPLA$_2$ε–GFP were surprisingly long (up to 30 µm) and resembled, from a morphological standpoint, tubular structures involved in the recycling of cargoes internalized through the clathrin-independent endocytic route driven by ARF6 GTPase (Naslavsky et al., 2003; Weigert et al., 2004). This transport route (referred to here as the clathrin-independent pathway) has been shown to operate the internalization and recycling of many clathrin-independent cargo proteins such as MHC-I, β-integrins and the GPI-anchored protein CD59, for example (Donaldson et al., 2009; Grant and Donaldson, 2009).

The HeLa cell line has been established as a model system to investigate transport through the clathrin-independent endocytic/recycling pathway (Donaldson et al., 2009; Grant and Donaldson, 2009). Therefore, to test the association of cPLA$_2$ε with this trafficking route, HeLa cells expressing cPLA$_2$ε–GFP were stained with antibodies against MHC-I. Confocal microscopy revealed substantial overlap of MHC-I and cPLA$_2$ε at the cell surface, as well as along intracellular tubular and vacuolar elements (Fig. 1A). The same colocalization pattern of cPLA$_2$ε was also detected for ARF6 (Fig. 1B) and other cargo following this clathrin-independent route, such as CD147 (Eyster et al., 2009). Tubular elements highlighted by cPLA$_2$ε also contained Rab22 and EHD1 (Fig. 1C), which have both been reported to operate in the recycling of clathrin-independent cargoes (Caplan et al., 2002; Weigert et al., 2004). In contrast, markers of the other endocytic compartments and Golgi residents exhibited significantly lower overlap with cPLA$_2$ε (Fig. 1D–I). The use of different tags (GFP, Myc or mCherry) affected neither the intracellular distribution pattern of cPLA$_2$ε nor the extent of its overlap with each of the above markers. Notably, strong overexpression of cPLA$_2$ε induced tubulation of clathrin-independent endocytic compartments labeled with MHC-I, whereas the overall distribution of other markers of early and late endocytic organelles remained unaffected (supplementary material Fig. S1). Thus, taken together, colocalization experiments suggest specific association of cPLA$_2$ε with the membrane compartments of the clathrin-independent endocytic/recycling pathway.

To further prove this point, we loaded cells with different endocytic tracers that highlight several specific uptake and recycling pathways. Internalization of fluorescent anti-MHC-I antibody was used to label the clathrin-independent route (Naslavsky et al., 2003), whereas uptake of transferrin or EGF was used to reveal clathrin-dependent recycling or degradative pathways, respectively. Again, preferential targeting of cPLA$_2$ε to the membrane compartments loaded with endocytosed MHC-I was detected (supplementary material Fig. S2A), whereas the enzyme association with endocytosed EGF and transferrin receptor was quite limited (supplementary material Fig. S2B,C). Finally, we tested whether cPLA$_2$ε was exclusively associated with the distal (recycling) compartments of the clathrin-independent route (as revealed by colocalization with Rab22 and EHD1) or could also be detected at the early incoming clathrin-independent endocytic structures. To this end, we used expression of ARF6$^{Q67L}$ as a tool to arrest clathrin-independent trafficking at the level of very early clathrin-independent endosomes, which appear as large and easily detectable vacuoles in cells (Naslavsky et al., 2003). Confocal microscopy revealed cPLA$_2$ε at the surface of such giant ARF6$^{Q67L}$ endosomes (supplementary material Fig. S2D; see also Fig. 3D), suggesting that the enzyme is also associated with early (incoming) membranes of the clathrin-independent pathway.

The intracellular distribution of cPLA$_2$ε was further investigated using immunoelectron microscopy. To better understand the identity of the structures containing cPLA$_2$ε, cells were loaded with anti-MHC-I antibody to label membranes of the clathrin-independent pathway. Double immunogold staining revealed both cPLA$_2$ε and MHC-I along the plasma membrane (Fig. 2A) and in the endosomes that contained few (<9) intraluminal vesicles (Fig. 2B) and therefore could be qualified as 'early endosomes' on the basis of their ultrastructural features (Saftig and Klumperman, 2009). Association of cPLA$_2$ε with the early clathrin-independent endocytic compartment was further confirmed because the enzyme was detected at the surface of the early clathrin-independent endosomes that accumulated in

Journal of Cell Science (2014) 127, 977–993 doi:10.1242/jcs.136598

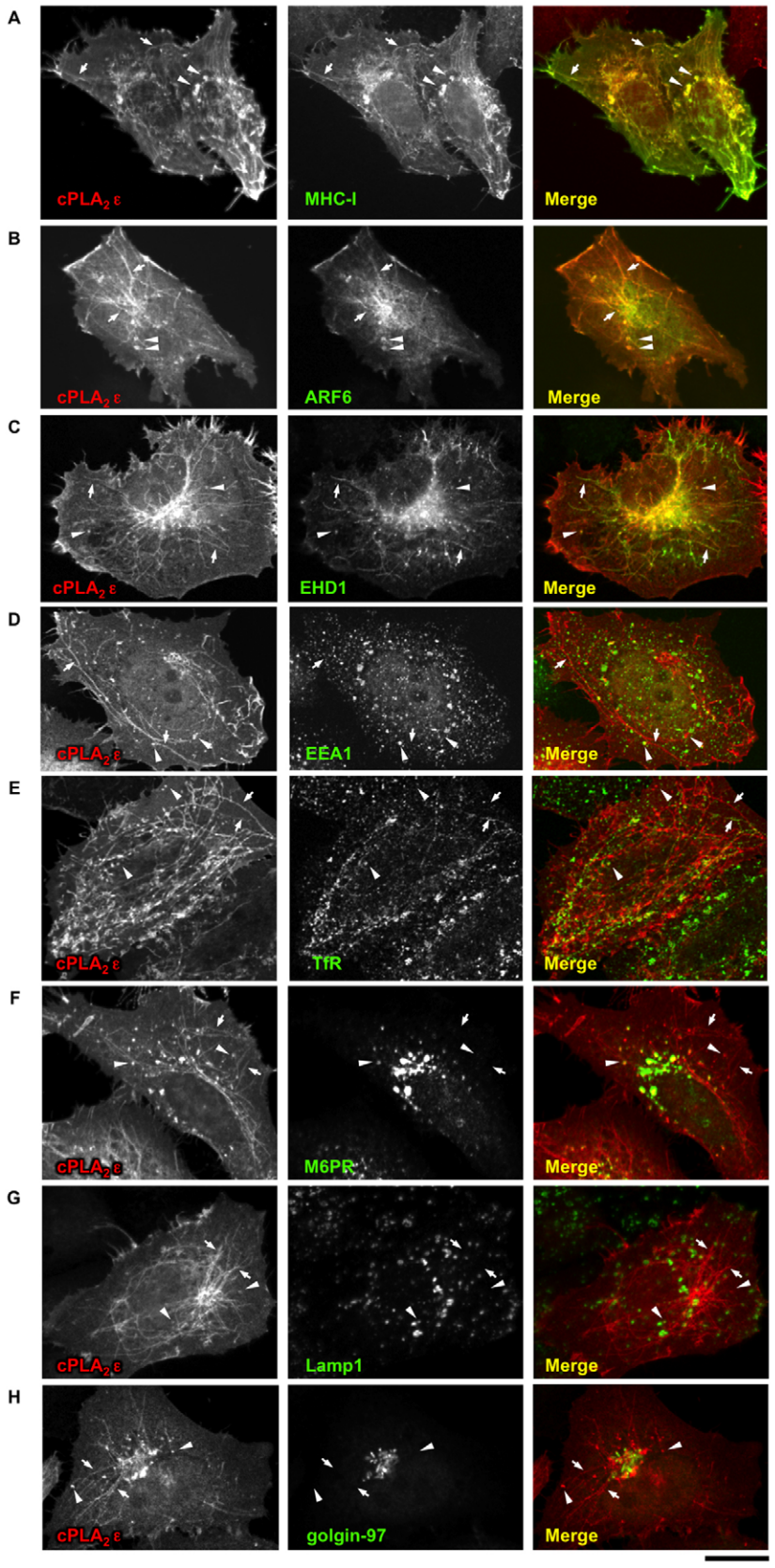


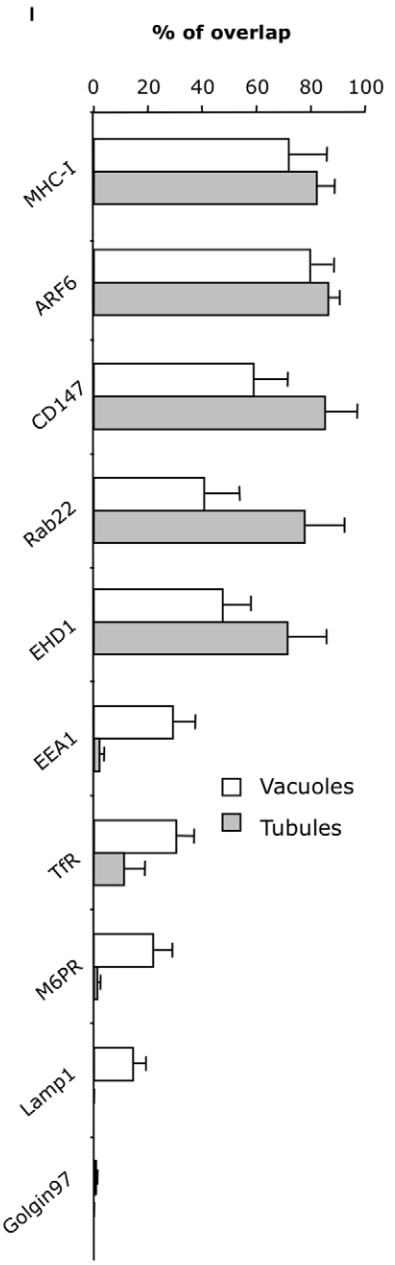


**Fig. 1. Intracellular localization of cPLA$_2$ε.** HeLa cells were transfected with either Myc–cPLA$_2$ε (A,B,F,G,H) or GFP–cPLA$_2$ε (C–E). ARF6-HA (B) and EHD1–Myc (C) were co-transfected with cPLA$_2$ε constructs. Cells were then fixed and labeled with anti-Myc antibody to reveal cPLA$_2$ε (A,B,F,G,H) or EHD1 (C), anti-HA antibody to label ARF6 (B) and antibodies against endogenously-expressed MHC-I (A), EEA1 (D), TfR (E), MPR (F), Lamp1 (G) and golgin-97 (H). After immunofluorescent labeling, the cells were analyzed under confocal microscope to evaluate cPLA$_2$ε colocalization with the above markers. Arrows and arrowheads in A–H indicate cPLA$_2$ε-positive tubules and vacuoles, respectively. (I) Morphometric analysis shows the percentage (means ± s.d., $n$=30 cells) of either vacuolar or tubular cPLA$_2$ε structures that exhibit overlap with other markers indicated. Scale bar: 5 μm.

Journal of Cell Science (2014) 127, 977–993 doi:10.1242/jcs.136598

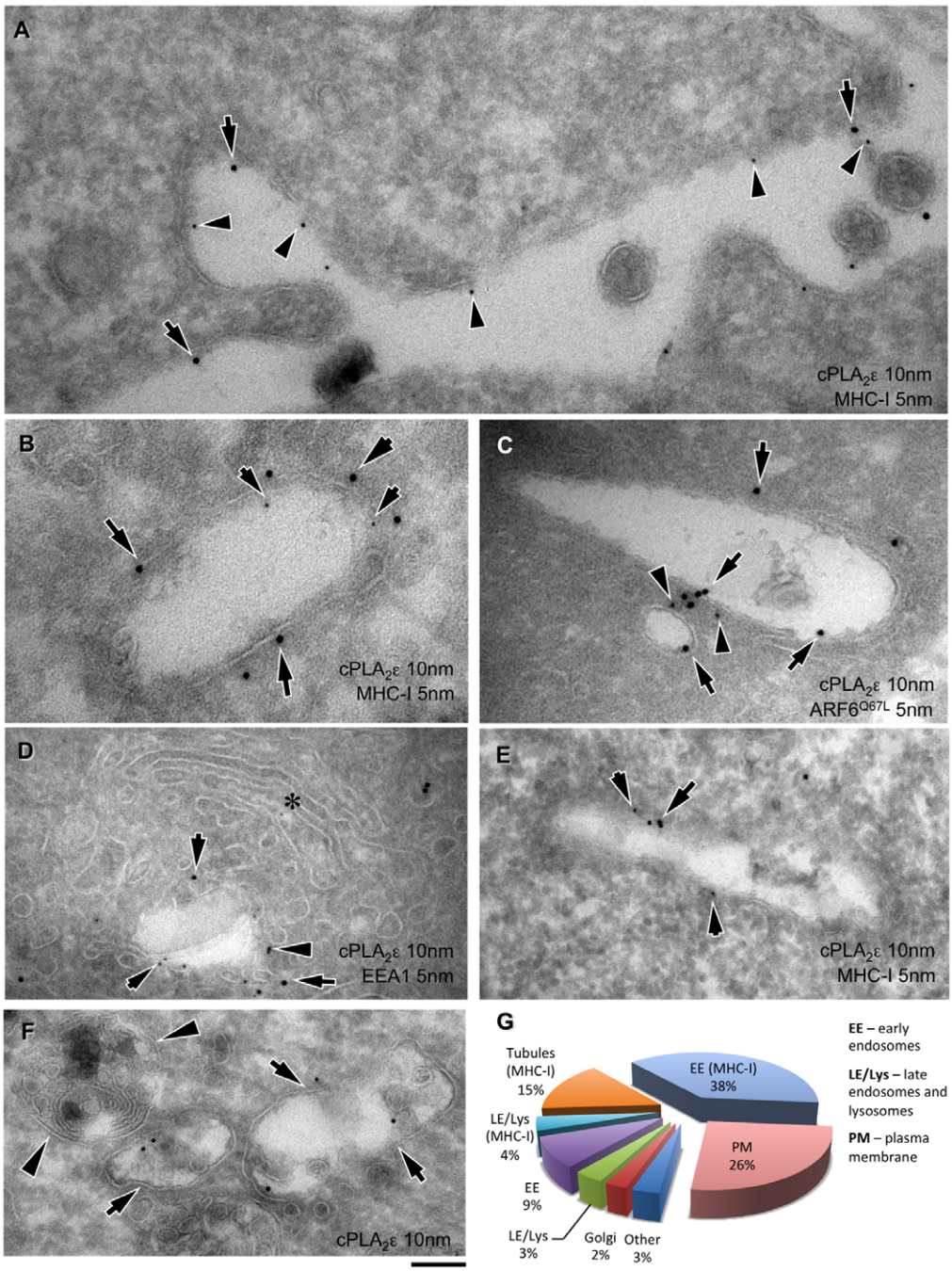


**Fig. 2. Immuno-EM labeling reveals cPLA$_2$ε association with compartments of the clathrin-independent pathway.** HeLa cells were transfected with either Myc–cPLA$_2$ε (A,B,E,F) or GFP–cPLA$_2$ε (C,D). ARF6$^{Q67L}$-HA (C) was co-transfected with cPLA$_2$ε. Cells shown in A,B,E were also loaded with Alexa-Fluor-488-conjugated antibody against MHC-I for 1 hour to label the membranes of the clathrin-independent transport route. Then cells were fixed, frozen and sectioned as described in the Materials and Methods. Sections were labeled with either anti-Myc (A,B,E,F) or anti-GFP (C,D) antibody to reveal cPLA$_2$ε, with anti-HA antibody to detect ARF6$^{Q67L}$-HA (C), anti-Alexa-Fluor-488 antibody to reveal internalized MHC-I (A,B,E) and with anti-EEA1 to label endogenous EEA1 (D). Arrows and arrowheads indicate cPLA$_2$ε and MHC-I, respectively, at the plasma membrane (A) and within the same early endosome (B). In C, cPLA$_2$ε (arrows) and ARF6$^{Q67L}$ (arrowheads) were detected at the surface of the same endocytic structures. In D, arrows indicate cPLA$_2$ε associated with structures decorated by EEA1 (arrowheads) while the membranes of Golgi stack (asterisk) lack cPLA$_2$ε labeling. (E) Tubular structure with internalized MHC-I (arrowheads) exhibited cPLA$_2$ε (arrow) at its surface. (F) cPLA$_2$ε signal is associated with early endosomes (arrows) that contained few intraluminal vesicles whereas late endosome/lysosome-like structures remained unlabeled (arrowheads). (G). Morphometric analysis of cells labeled for both cPLA$_2$ε and internalized MHC-I shows the percentage of cPLA$_2$ε-associated gold particles in different compartments. MHC-I in parentheses indicates MHC-I-positive organelles. Scale bar: 120 nm (A–C), 180 nm (D–F).

the cells upon overexpression of ARF6$^{Q67L}$ (Fig. 2C). We also found that the subpopulation of cPLA$_2$ε-positive structures contained EEA1 (Fig. 2D), an early endosomal marker, which binds to the surface of clathrin-independent endosomes during their maturation and shortly before their convergence with the clathrin-dependent endocytic pathway (Naslavsky et al., 2003). In addition to typical vacuolar endocytic structures, cPLA$_2$ε decorated 50- to 200-nm-thick tubular elements that contained internalized MHC-I (Fig. 2E) and resembled, from the ultrastructural standpoint, clathrin-independent recycling tubules described previously (Caplan et al., 2002). cPLA$_2$ε labeling was quite specific, because the late endosomes with numerous intraluminal vesicles (Fig. 2F, arrowheads) and the Golgi membranes (Fig. 2D, asterisk), exhibited little or no cPLA$_2$ε at their surface (see also quantification in Fig. 2G). Such a distribution of the cPLA$_2$ε labeling was consistent with poor colocalization of the enzyme with either lysosomal or Golgi markers (see Fig. 1) in immunofluorescence, and indicates a specific association of cPLA$_2$ε with incoming and recycling compartments of the clathrin-independent transport route.

### The C-terminal cluster of basic amino acids defines targeting of cPLA$_2$ε to the clathrin-independent endocytic/recycling pathway

Most of the enzymes from the cPLA$_2$ family are thought to rely on the N-terminal $Ca^{2+}$-binding (C2) domain for the membrane binding that occurs upon an increase of $Ca^{2+}$ in the cytosol (Ghosh et al., 2006b). The specific properties of the given C2 domain have been reported to define the preference of its own

Journal of Cell Science (2014) 127, 977–993 doi:10.1242/jcs.136598

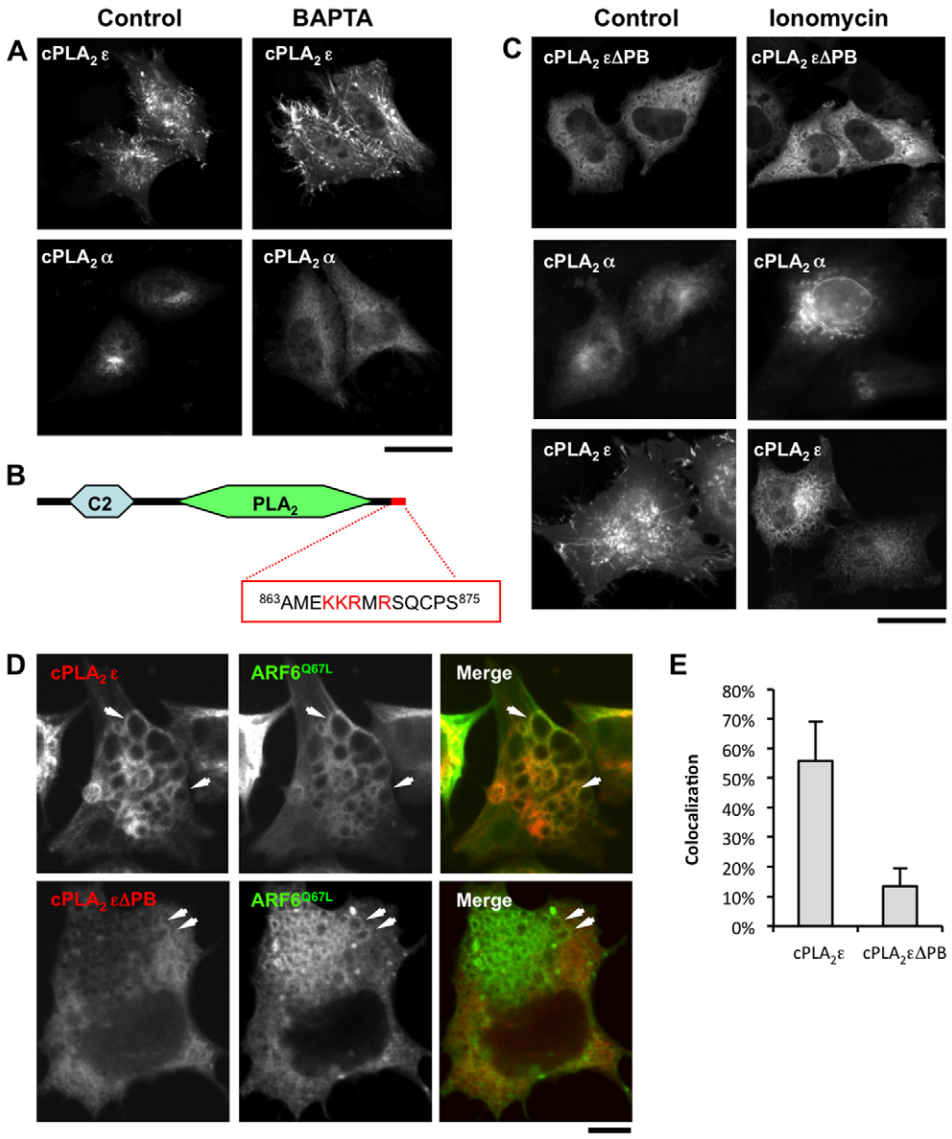


**Fig. 3. $cPLA_2\varepsilon$ and $cPLA_2\alpha$ show different sensitivity to a variation of cytosolic $Ca^{2+}$ concentration.** (A) HeLa cells were transfected with GFP–$cPLA_2\alpha$ or GFP–$cPLA_2\varepsilon$ cDNAs (as indicated) and fixed directly (left column) or 30 minutes after addition of 20 μM $Ca^{2+}$ chelator BAPTA (right column). $Ca^{2+}$ reduction induced detachment of $cPLA_2\alpha$ from the Golgi membranes into the cytosol but did not affect localization of $cPLA_2\varepsilon$, which remains membrane associated. (B) Schematic representation of $cPLA_2\varepsilon$ protein and its C-terminal cluster of basic amino acids. The analysis of mouse $cPLA_2\varepsilon$ sequence revealed the presence of a polybasic (PB) cluster of four positively charged residues (red letters) at the end of C-terminal part of the enzyme. (C) HeLa cells expressing Myc–$cPLA_2\varepsilon\Delta PB$, GFP–$cPLA_2\alpha$ and Myc–$cPLA_2\varepsilon$ cDNAs (as indicated on single panels) were fixed directly (left column) or 10 minutes after incubation with 10 μM $Ca^{2+}$ ionophore ionomycin (right column) and stained with anti-Myc to reveal $cPLA_2\varepsilon\Delta PB$ or $cPLA_2\varepsilon$. $cPLA_2\varepsilon\Delta PB$ exhibited a mostly cytosolic pattern even when ionomycin was added to the cells. In contrast, ionomycin significantly improved association of $cPLA_2\alpha$ with perinuclear Golgi and ER membranes. Conversely, full-length $cPLA_2\varepsilon$ was displaced by ionomycin from the plasma membrane and intracellular tubular-vacuolar structures into the cytosol. (D) HeLa cells were co-transfected with either Myc–$cPLA_2\varepsilon$ and $ARF6^{Q67L}$ (top row) or Myc–$cPLA_2\varepsilon\Delta PB$ and $ARF6^{Q67L}$ (bottom row). The cells were fixed, permeabilized and labeled with anti-ARF6 and anti-Myc antibodies. Overexpression of $ARF6^{Q67L}$ induced formation of large vacuoles (arrows) where $cPLA_2\varepsilon$ (top row) but not $cPLA_2\varepsilon\Delta PB$ (bottom row) was recruited. (E) Quantification revealed a decrease in colocalization (means ± s.d., $n=30$ cells) of $cPLA_2\varepsilon\Delta PB$ with $ARF6^{Q67L}$ when compared with full-length $cPLA_2\varepsilon$. Scale bar: 8 μm (A,C), 4 μm (D).

protein (comprising $cPLA_2$ enzymes) for specific membrane compartments (Evans et al., 2004). In this context, we wanted to check to what extent the $Ca^{2+}$ and C2 domain contribute to $cPLA_2\varepsilon$ specificity for the clathrin-independent pathway. HeLa cells expressing $cPLA_2\varepsilon$ were treated with the $Ca^{2+}$ chelator BAPTA to deplete cytosolic $Ca^{2+}$. In parallel, $Ca^{2+}$-sensitive $cPLA_2\alpha$ was used as a control to check the effectiveness of BAPTA treatment.

Confocal microscopy revealed that a substantial pool of $cPLA_2\varepsilon$ could be detected at the plasma membrane and at intracellular structures in untreated cells (Fig. 3A). Incubation with BAPTA did not significantly change the intracellular pattern of $cPLA_2\varepsilon$ (Fig. 3A). This behavior of $cPLA_2\varepsilon$ upon depletion of $Ca^{2+}$ was strikingly different from that of $cPLA_2\alpha$ that was displaced completely from the Golgi into the cytosol after the addition of BAPTA (Fig. 3A). These observations argued against the essential role of the $Ca^{2+}$ and C2 domain of $cPLA_2\varepsilon$ in the recruitment of this enzyme to clathrin-independent membranes.

This prompted us to further investigate whether any other specific targeting motif could be found in $cPLA_2\varepsilon$. Sequence analysis of $cPLA_2\varepsilon$ revealed a stretch of basic amino acids (865KKRMR870) located almost at the end of its C-terminus (see Fig. 3B). Interestingly, such polybasic (PB) clusters have been reported in many proteins to allow plasma membrane binding through interaction with $PI(4,5)P_2$ and/or $PI(3,4,5)P_3$ (Heo et al., 2006). Thus, a DNA construct encoding truncated $cPLA_2\varepsilon$ (hereafter referred to as $cPLA_2\varepsilon\Delta PB$), which lacks the last 10 C-terminal amino acids comprising the basic cluster was prepared and its intracellular distribution was investigated. Deletion of the PB domain resulted in displacement of the protein from the membranes (Fig. 3C), indicating that this motif is the main determinant that defines $cPLA_2\varepsilon$-specific targeting towards clathrin-independent compartments.

At this point we reasoned that regardless of the dominant role of the PB cluster in $cPLA_2\varepsilon$ targeting, the C2 domain could still be used by the enzyme for membrane binding under certain conditions (when the PB domain is inactive, for example). To test whether this is the case, cells expressing $cPLA_2\varepsilon\Delta PB$ were treated with ionomycin, an ionophore that increases cytosolic $Ca^{2+}$. Despite the presence of the C2 domain, $cPLA_2\varepsilon\Delta PB$ did not exhibit any significant shift from the cytosol towards the plasma membrane or any intracellular membranes (Fig. 3C), whereas in

Journal of Cell Science (2014) 127, 977–993 doi:10.1242/jcs.136598

control experiments, the effectiveness of ionomycin treatment was confirmed by a significant recruitment of $Ca^{2+}$-sensitive cPLA$_2$α to the Golgi and ER membranes and its reduction in the cytosol (Fig. 3C). Interestingly, addition of the ionomycin induced partial loss of the full-length cPLA$_2$ε from the plasma membrane and some clathrin-independent membranes comprising recycling tubules (Fig. 3C). Such behavior of cPLA$_2$ε was not expected for the protein with the C2 domain, but would have been likely for the protein with the PB motif. Given that the PB domain uses PI(4,5)P$_2$ as the main ligand (Heo et al., 2006), the hydrolysis of this lipid by PLC upon addition of ionomycin (Heo et al., 2006) is likely to reduce binding of cPLA$_2$ε to the membrane.

To further check whether PI(4,5)P$_2$ is involved in cPLA$_2$ε recruitment to the membranes we used ARF6$^{Q67L}$ as a tool to generate PI(4,5)P$_2$-enriched membranes. As mentioned above, ARF6$^{Q67L}$ induces accumulation of giant clathrin-independent endosomes. Importantly, such ARF6$^{Q67L}$-positive endosomes have been reported to contain high amounts of PI(4,5)P$_2$ (Naslavsky et al., 2003). Confocal microscopy revealed cPLA$_2$ε along the membranes of such ARF6$^{Q67L}$ vacuoles, whereas deletion of the PB domain resulted in dissociation of the enzyme from these PI(4,5)P$_2$-enriched structures (Fig. 3D,E).

In the context of the above observations and the reported affinity of the PB domain for PI(4,5)P$_2$ and PI(3,4,5)P$_3$ (Heo et al., 2006), we checked the lipid-binding properties of cPLA$_2$ε in a lipid overlay assay. To this end, recombinant GST-tagged cPLA$_2$ε, its C-terminus (815–875 respectively) and cPLA$_2$εΔPB were purified and spotted on PIP strips (see the Materials and Methods). In control experiments, GST alone did not interact with any lipid in the strips, whereas GST-fused probes for PI(3)P (p40-PX domain), PI(4)P (C-terminal fragment of *Legionella pneumophila* SidC protein) and PI(4,5)P$_2$ (PLCδ-PH domain) bound corresponding lipids with high specificity (Fig. 4A). Furthermore, we found that both full-length cPLA$_2$ε and its C-terminal peptide exhibited a substantial interaction with different phosphoinositides comprising PI(4,5)P$_2$, whereas the cPLA$_2$εΔPB did not show any significant affinity for any of the tested lipids, such as the negative GST control (Fig. 4A). Interestingly, cPLA$_2$ε was found to interact with all PIPs at a similar magnitude, and in addition, exhibited a substantial affinity for phosphatidic acid (PA), which might be used by the enzyme as a substrate. However, the C-terminal PB domain of the cPLA$_2$ε did not interact with PA and PI(3)P, and its binding to remaining PI mono-phosphates was significantly lower than to bis- and tris-phosphates. This suggests that the PB domain renders full-length cPLA$_2$ε to a conformation that strengthens its interaction with PA and PI(3)P *in vitro*.

Given that *in vitro* cPLA$_2$ε exhibited quite promiscuous interaction with different PIP species, we sought to investigate how it binds *in vivo* to membranes enriched in specific PIPs. To this end, we evaluated the intracellular colocalization of cPLA$_2$ε with PIP-binding probes such as PH domains of PLCδ (PLCδ-PH), CERT (CERT-PH), GRP1 (GRP1-PH) and FIVE domain of SARA (SARA-FIVE) that have a high affinity for PI(4,5)P$_2$, PI(4)P, PI(3,4,5)P$_3$ and PI(3)P, respectively. Confocal microscopy revealed substantial colocalization of PLCδ-PH with cPLA$_2$ε along tubular and some vacuolar structures (Fig. 4B), indicating that the enzyme efficiently binds to PI(4,5)P$_2$-enriched membranes *in vivo*. Interestingly, strong overexpression of PLCδ-PH frequently induced a detachment of cPLA$_2$ε from the membranes (Fig. 4C), indicating that there is competition of the proteins for the same PI(4,5)P$_2$ binding site. In contrast, cPLA$_2$ε exhibited an almost complete lack of overlap with the PI(4)P-specific CERT-PH, which was mainly distributed over the Golgi (Fig. 4D). Colocalization of the enzyme with GRP1-PH, which binds to PI(3,4,5)P$_3$, was mainly restricted to the plasma membrane, and in some cases, the tips of the recycling tubules (Fig. 4E). Interestingly, a clear cPLA$_2$ε signal was detected over the SARA-FYVE-positive endosomes (Fig. 4F), suggesting that the enzyme was able to bind to PI(3)P membranes. However, incubation with wortmannin [an inhibitor of the phosphatidylinositol and therefore 3-kinase PI(3)P synthesis] did not change the intracellular pattern of cPLA$_2$ε, whereas the same treatment induced detachment of the PI(3)P-binding proteins (such as EEA1) from the endosomal membranes into the cytosol (not shown). This suggests that recruitment of cPLA$_2$ε to the SARA-FYVE membranes did not rely exclusively on its interaction with PI(3)P and that alternative binding mechanisms might exist. Indeed, cPLA$_2$ε did not appear to compete with SARA-FYVE for PI(3)P-binding sites because overexpression of SARA-FYVE did not displace the enzyme from the membranes (not shown). Therefore, taken together, the above experiments indicate that the specific association of cPLA$_2$ε with the membrane organelles of the clathrin-independent pathway relies on the interaction of the C-terminal PB domain of the enzyme with PI(4,5)P$_2$.

### Depletion of cPLA$_2$ε affects recycling through the clathrin-independent pathway

The specific targeting of cPLA$_2$ε to the clathrin-independent endocytic/recycling route suggests that the enzyme is involved in the regulation of the transport events in this pathway. To test whether this is the case, we first used an RNAi approach. Although the anti-cPLA$_2$ε antibody failed to label the endogenous enzyme in immunofluorescence experiments, in western blots the antibody recognized a ~96 kDa band corresponding to the molecular mass of cPLA$_2$ε. This band was significantly reduced in HeLa cells that were incubated with cPLA$_2$ε-specific siRNA(s), indicating the sufficient efficiency of the silencing (Fig. 5A).

To understand whether cPLA$_2$ε depletion has an impact on the organization of clathrin-independent pathway we first stained control and silenced cells for MHC-I. Confocal microscopy revealed a significant increase in the MHC-I-associated fluorescent signal in the perinuclear area upon cPLA$_2$ε knock down (Fig. 5B, arrowheads), indicating that the recycling of MHC-I from the perinuclear compartment back to the cell surface might be delayed upon depletion of cPLA$_2$ε. Indeed, expression of mouse cPLA$_2$ε (that is resistant to human cPLA$_2$ε-specific siRNAs) in silenced cells significantly reduced MHC-I accumulation in the perinuclear compartment (Fig. 5B, asterisks), probably by rescue of MHC-I recycling back to the plasma membrane.

Recycling through the clathrin-independent route has been reported to rely on the formation of long tubular elements that serve as precursors for the formation of transport carriers directed to the surface of the cells (Grant and Donaldson, 2009). In this context, we checked whether silencing of cPLA$_2$ε affects the formation of such long tubular elements given that PLA$_2$ activity has been demonstrated to facilitate the formation of the membrane tubules, in both the secretory and endocytic pathways (Bechler et al., 2012; Ha et al., 2012). Confocal microscopy of the control cells frequently revealed several MHC-I tubular elements emerging from the perinuclear area (Fig. 5C,

Journal of Cell Science (2014) 127, 977–993 doi:10.1242/jcs.136598

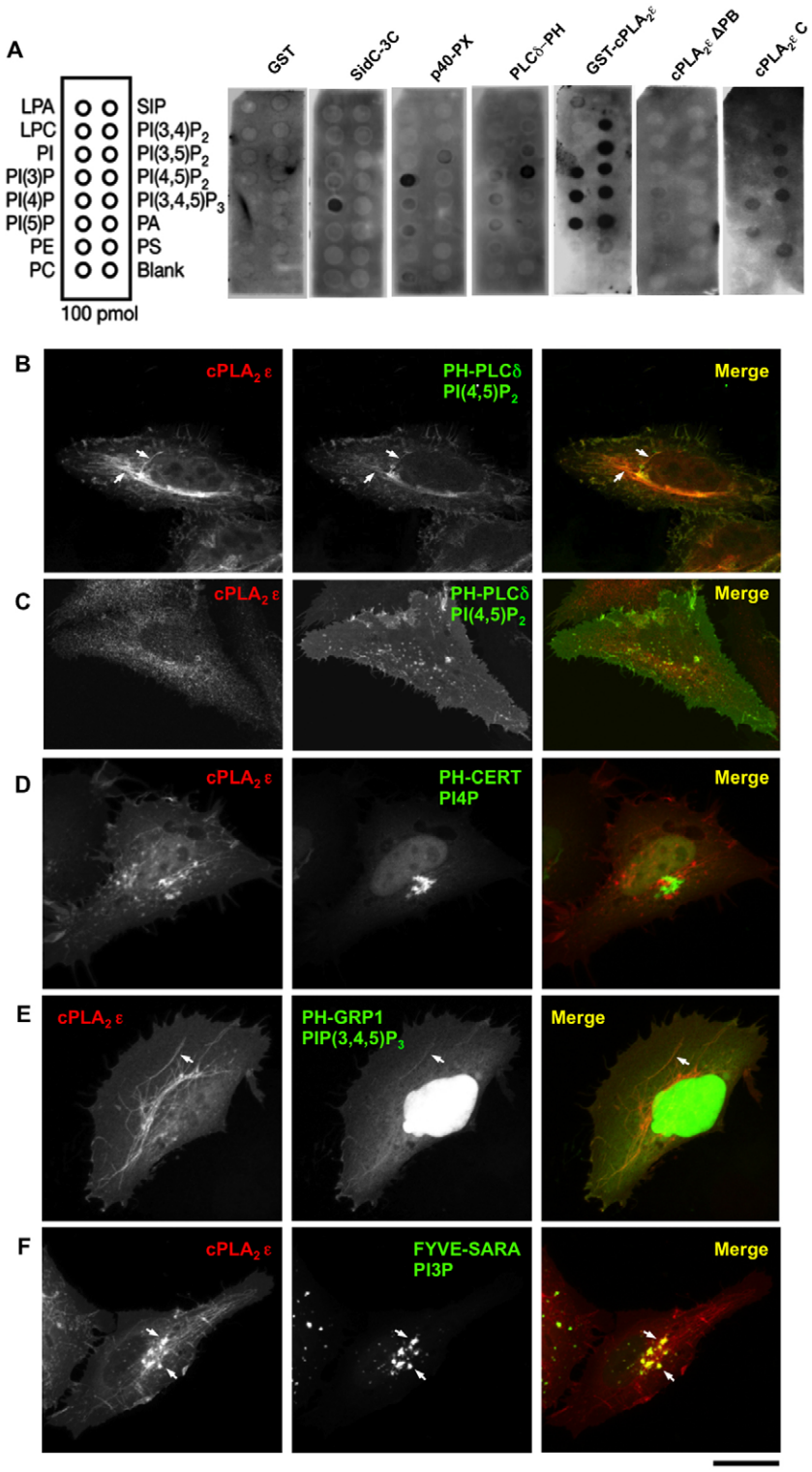


**Fig. 4. Association of cPLA$_2$ε with phosphatidylinositol lipids.** (A) PIP strip membranes containing spotted phosphatidylinositols and other lipids (as indicated in scheme) were incubated with 5 μg/ml of the following recombinant proteins: GST alone, GST–SidC-3C, GST–p40-PX, GST–PH-PLCδ, GST–cPLA$_2$ε full-length, GST–cPLA$_2$ε N-terminus (amino acids 1–63), GST–cPLA$_2$ε C-terminus (815–875) and GST–cPLA$_2$ε full-length fusion proteins. Then the membranes were washed and the proteins bound to the lipids were determined by immunoblotting with an anti-GST antibody. GST alone and GST–cPLA$_2$ε N-terminus did not exhibit binding to any of the lipids. As expected, GST–SidC-3C, GST–p40-PX and GST–PH-PLCδ were bound to PI(4)P, PI(3)P and PI(4,5)P$_2$, respectively. GST–cPLA$_2$ε C-terminus and GST–cPLA$_2$ε remained bound to different PIPs. GST–cPLA$_2$ε binding to PA was also detected. (B–F) HeLa cells were co-transfected with cDNAs encoding Myc–cPLA$_2$ε and GFP-tagged PI-binding probes PH-PLCδ (B,C), PH-CERT (D), PH-GRP1 (E) and FIVE-SARA (F). The cells were then fixed and labeled with anti-Myc antibody. cPLA$_2$ε exhibited substantial overlap with PH-PLCδ (B, arrows) and was displaced from the membranes in cells overexpressing PH-PLCδ (C). No overlap of cPLA$_2$ε with PH-CERT was detected (D). PH-GRP1 was revealed at the tips of few cPLA$_2$ε-positive tubules (E, arrows). FIVE-SARA was bound only to the vacuolar cPLA$_2$ε structures (F, arrows) whereas cPLA$_2$ε tubules remained devoid of the FIVE-SARA signal (F). Scale bar: 4.5 μm (B–F).

arrows). Both the length and the number of such tubular structures were reduced by knockdown of cPLA$_2$ε (Fig. 5C–E). In contrast, overexpression of cPLA$_2$ε (about four times above the endogenous level) induced the opposite phenotype, with a compelling increase in MHC-I tubular elements (Fig. 5C–E).

To prove the involvement of cPLA$_2$ε in the regulation of the transport through the clathrin-independent route, MHC-I uptake and recycling assays were used. First, we determined the impact of cPLA$_2$ε depletion on the internalization of MHC-I. Confocal microscopy revealed that the amount of endocytosed MHC-I was similar in control and silenced cells at the early time points (i.e. within 10 minutes) after activation of endocytosis (Fig. 5F). This suggests that depletion of cPLA$_2$ε did not affect early stages of the internalization in the clathrin-independent endocytic pathway. However, we noted that with time (after 15–20 minutes), the intracellular MHC-I pool tended to increase in silenced cells

Journal of Cell Science (2014) 127, 977–993 doi:10.1242/jcs.136598

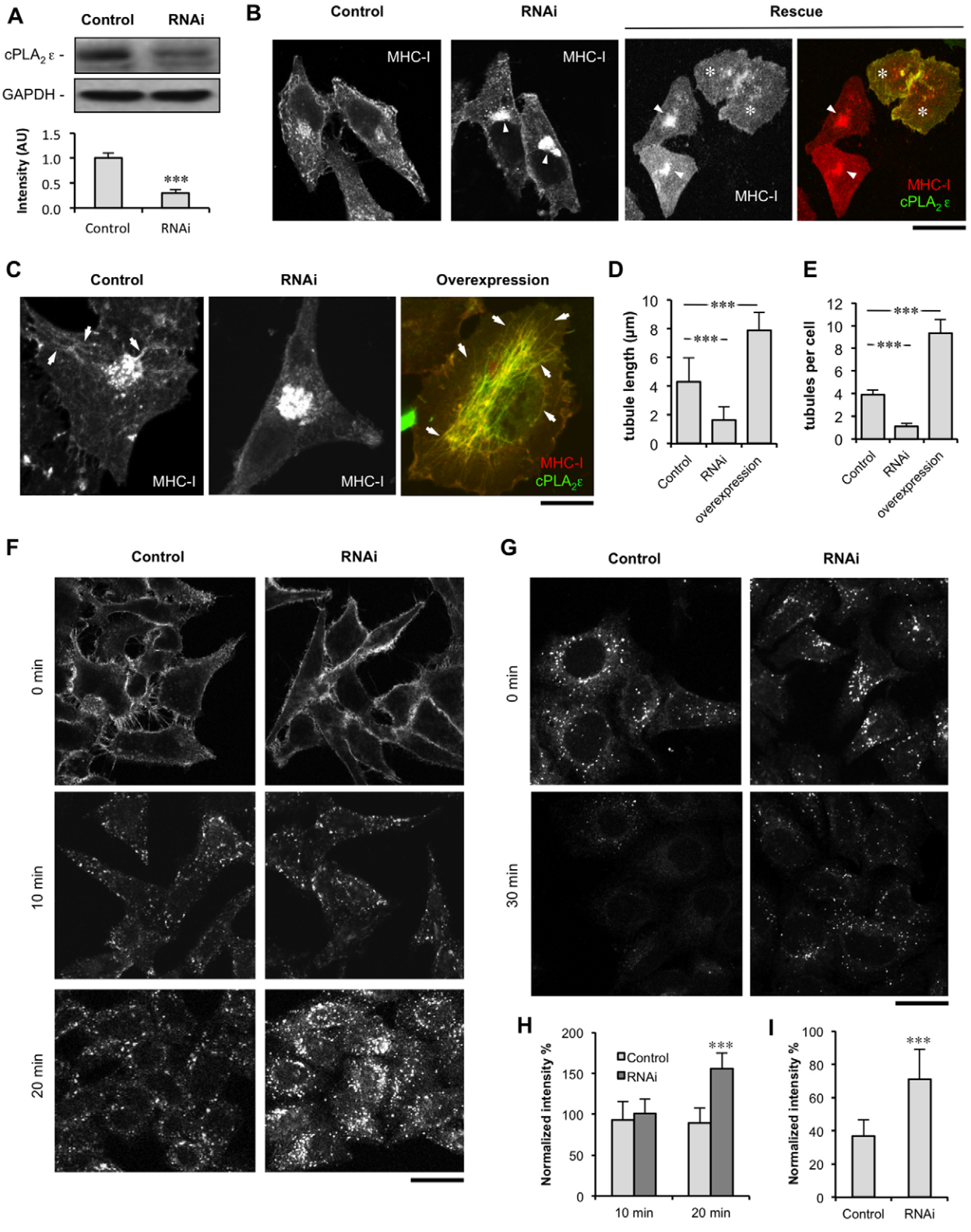


**Fig. 5.** See next page for legend.

(Fig. 5F), which was probably due to an impairment of the MHC-I recycling back to the cell surface.

To test whether this was the case we used cytochalasin D, which has been reported to block and therefore synchronize internalized MHC-I within the clathrin-independent recycling compartment (Weigert et al., 2004). Indeed, cytochalasin D treatment allowed similar amounts of MHC-I to accumulate over 30 minutes in control and cPLA$_2$ε-silenced cells (Fig. 5G), indicating that depletion of cPLA$_2$ε did not impact MHC-I internalization. Next, the drug was removed to trigger MHC-I

Journal of Cell Science (2014) 127, 977–993 doi:10.1242/jcs.136598

**Fig. 5. $cPLA_2\varepsilon$ silencing affects tubule formation and recycling in the clathrin-independent pathway.** (A) HeLa cells were treated with either scramble or $cPLA_2\varepsilon$-specific siRNAs for 96 hours, lysed and subjected to immunoblotting with antibodies against either $cPLA_2\varepsilon$ or GAPDH. The anti-$cPLA_2\varepsilon$ antibody recognized a ~96 kDa band that corresponded to the molecular mass of $cPLA_2\varepsilon$ and was significantly reduced in $cPLA_2\varepsilon$-silenced cells as also revealed by quantification (see graph). (B) HeLa cells were treated with scramble or $cPLA_2\varepsilon$-specific siRNAs or transfected with the mouse GFP–$cPLA_2\varepsilon$ cDNA 72 hours after addition of $cPLA_2\varepsilon$-specific siRNA (indicated as Rescue). After 96 hours of siRNA treatment, cells were fixed and labeled with anti-MHC-I antibody. $cPLA_2\varepsilon$-silenced cells exhibited strong perinuclear MHC-I accumulations (arrowheads), which disappeared almost completely in cells overexpressing $cPLA_2\varepsilon$ (asterisks). (C–E) HeLa cells were subjected to either $cPLA_2\varepsilon$ RNAi or to overexpression of the enzyme, fixed and investigated using confocal microscopy to analyze frequency and length of MHC-I tubular structures (indicated by arrows). Significant reduction of MHC-I-containing tubules was detected in cells incubated with siRNA, whereas $cPLA_2\varepsilon$ overexpression induced strong tabulation of MHC membranes (C, arrows). The graphs in D and E show a reduction in the length of MHC-I tubules (means ± s.d., $n=30$ cells) and their number per cell (means ± s.d., $n=30$ cells), respectively, whereas the overexpression of the $cPLA_2\varepsilon$ induced a significant increase in length and number of tubular structures. (F) Control (left column) or $cPLA_2\varepsilon$-silenced (right column) cells were incubated for 30 minutes at 4°C with anti-MHC-I antibody to detect surface-bound MHC-I (see Materials and Methods) or incubated at 37°C for 10 minutes and 20 minutes and subjected to acid washing to reveal the internal pool of internalized MHC-I. Control and $cPLA_2\varepsilon$-depleted cells exhibited similar amounts of anti-MHC-I bound to the cell surface (top row) and internalized 10 minutes after activation of MHC-I uptake (middle row). In contrast, at 20 minutes, more internalized MHC-I was revealed in silenced cells, indicating a delay in MHC-I recycling. (G) Control and $cPLA_2\varepsilon$-depleted cells were incubated at 4°C with anti MHC-I antibody, washed and subjected to CytD block to inhibit MHC-I recycling back to the plasma membrane. Then the cells were washed with acid buffer and fixed directly (G, top row). Alternatively, the cells were incubated for 30 minutes at 37°C to allow MHC-I recycling (G, bottom row) and subjected to an acid wash before fixation. Immunofluorescence analysis revealed only the intracellular MHC-I pool, which remained significantly higher in $cPLA_2\varepsilon$-silenced cells. (H,I) Normalized fluorescent intensity of MHC-I (means ± s.d., $n=50$ cells) corresponding to uptake (F) and recycling (G) experiments respectively. ***$P<0.001$, Student's $t$-test. Scale bars: 8 μm (B,F), 4 μm (C), 7 μm (G).

recycling (Weigert et al., 2004). Fig. 5G shows that 30 minutes after activation of the recycling (cytochalasin D wash-out), almost all the MHC-I was transported away from the intracellular compartments in control cells. In contrast, $cPLA_2\varepsilon$-depleted cells still exhibited quite strong MHC-I staining associated with the intracellular membranes (Fig. 5G), indicating a delay in recycling through the clathrin-independent route. The accumulation of MHC-I in silenced cells was confirmed by morphometric analysis in both uptake and recycling experiments (Fig. 5H,I). Next, the MHC-I recycling in control and silenced cells was investigated under steady-state conditions (i.e. without cytochalasin D block). Similar to when the cytochalasin D block was released, $cPLA_2\varepsilon$ ablation induced retention of MHC-I in the clathrin-independent recycling compartment (supplementary material Fig. S3).

In addition, we checked whether $cPLA_2\varepsilon$ is engaged in the regulation of the transport events within other endocytic/recycling routes. We found that $cPLA_2\varepsilon$-depleted cells did not exhibit significant changes in the pattern of either M6PR or caveolin, suggesting that transport through endosome-to-Golgi or caveolin-dependent routes, respectively, does not require this enzyme (supplementary material Fig. S4A,B). Similarly, knock-down of $cPLA_2\varepsilon$ did not affect uptake and delivery of EGF to the late endocytic compartment (supplementary material Fig. S4C). When fluorescent transferrin (Tfn) was added to cells, the amount of internalized tracer remained almost the same in control and silenced cells at both early (10 minutes) and late (20 minutes) time intervals after the pulse (supplementary material Fig. S4D), indicating that neither uptake nor recycling of Tfn is affected by a deficit of $cPLA_2\varepsilon$.

Thus, taken together, the above results suggest that $cPLA_2\varepsilon$ operates mainly and quite specifically in transport through the clathrin-independent route. To further support this conclusion, we investigated the association of $cPLA_2\varepsilon$ with specific cargoes – CD55, CD98 and CD147 – that use the clathrin-independent uptake and recycling pathway (Eyster et al., 2009). All three proteins exhibited a substantial overlap with the enzyme along tubular elements and vesicular structures (Fig. 6A). Next, the impact of $cPLA_2\varepsilon$ depletion on CD55 and CD147 recycling was evaluated. Control and $cPLA_2\varepsilon$-silenced cells were uploaded with antibodies against either CD55 or CD147 in the presence of cytochalasin D to accumulate corresponding cargoes in the recycling clathrin-independent compartment. Cytochalasin D was then washed out to activate the recycling of either CD55 or CD147. Fig. 6B,C shows that in control cells, the intracellular pool of CD55 was consumed within 30 minutes after cytochalasin D washout as a result of recycling, whereas $cPLA_2\varepsilon$-deficient cells still retained a significant amount of internalized CD55. Similarly, $cPLA_2\varepsilon$ suppression induced intracellular retention of CD147 (Fig. 6D), indicating that the enzyme is required to support recycling of the specific cargoes through the clathrin-independent route.

### Catalytic activity of $cPLA_2\varepsilon$ is required to drive trafficking through the clathrin-independent recycling pathway

The recycling of the MHC-I and similar clathrin-independent endocytic cargoes back to the cell surface is mediated through tubular elements that serve as precursors for transport carriers carrying the cargo to the plasma membrane (Grant and Donaldson, 2009; Weigert et al., 2004). The formation of tubular membrane structures operating in several intracellular transport routes has been reported to require catalytic activity of $PLA_2$ enzymes (Bechler et al., 2011; Bechler et al., 2010; San Pietro et al., 2009). It has been hypothesized that phospholipid hydrolysis by $PLA_2$ enzymes results in an increase in wedge-shaped lysolipids that induce or support a high curvature of the tubule membrane (Bechler et al., 2012; Ha et al., 2012; Polishchuk et al., 2009). Thus we wondered whether the catalytic activity of $cPLA_2\varepsilon$ is needed for the generation of the tubular elements that support recycling of the MHC-I from the intracellular compartments back to the cell surface. Given that the specific chemical inhibitors for $cPLA_2\varepsilon$ are yet to be developed, we generated an inactive $cPLA_2\varepsilon$ protein. According to predictions (Ghosh et al., 2006b), an active site in $cPLA_2\varepsilon$ contains a nucleophilic serine (S420), which is conserved among different $cPLA_2$ enzymes (Fig. 7A) and should have a key role in $cPLA_2\varepsilon$ catalytic activity. Thus a $cPLA_2\varepsilon^{S420A}$ mutant was created and expressed in HEK293 cells to evaluate its catalytic activity. Fig. 7B shows that the mutant exhibited a reduced capacity to hydrolyze phospholipids compared with the wild-type $cPLA_2\varepsilon$ enzyme, although both $cPLA_2\varepsilon$ and $cPLA_2\varepsilon^{S420A}$ were expressed at the same level in the cells, as evaluated by western blot (not shown). Further analysis revealed that overexpression of $cPLA_2\varepsilon$ substantially increased the amount of lysolipids in the cells, whereas $cPLA_2\varepsilon^{S420A}$ failed to stimulate lysolipid production (Fig. 7C). Thus it turns out that the catalytic activity of the mutant was significantly reduced compared with the wild-type $cPLA_2\varepsilon$. Next, an inactive $cPLA_2\varepsilon^{S420A}$ mutant was

Journal of Cell Science (2014) 127, 977–993 doi:10.1242/jcs.136598

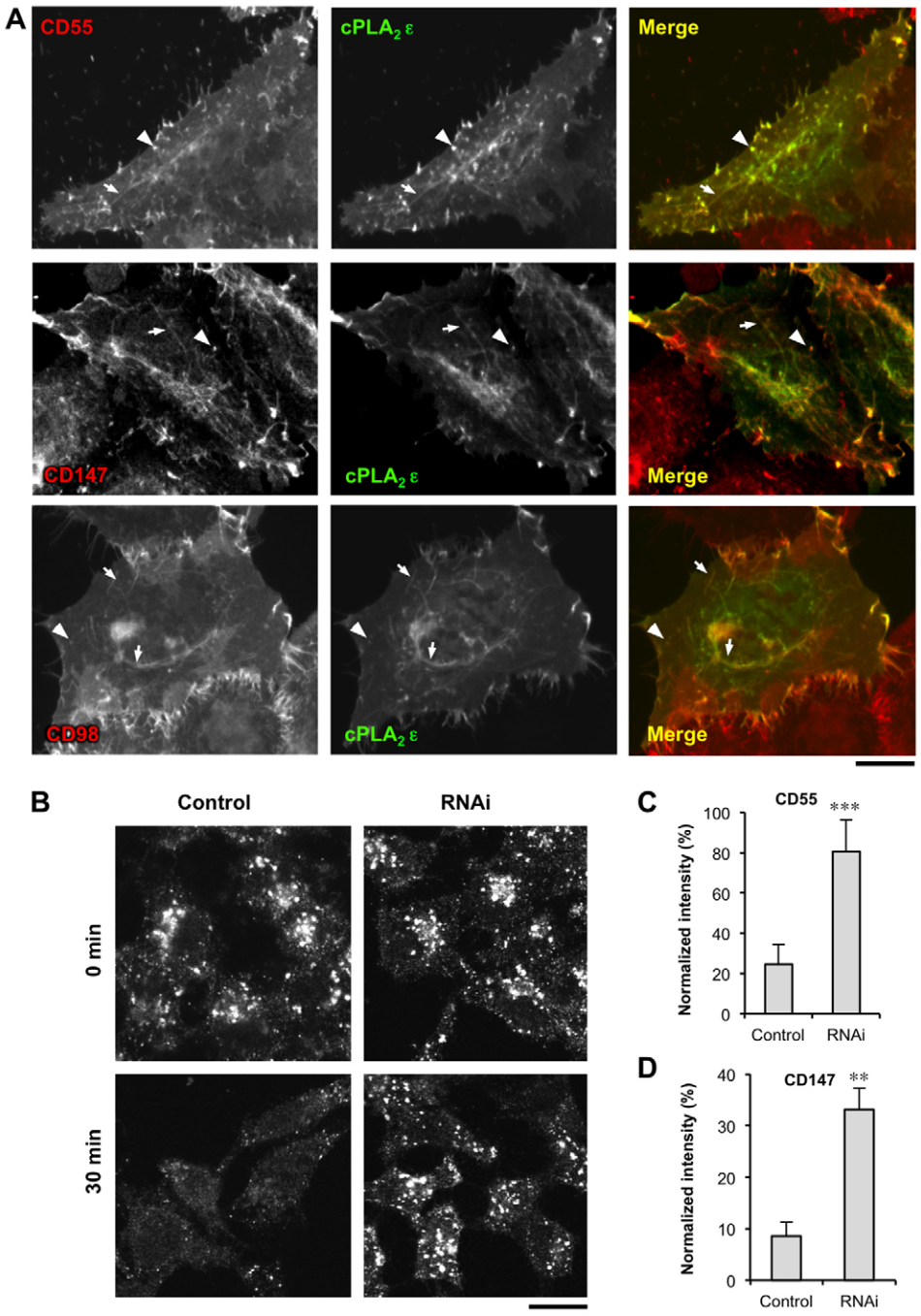


**Fig. 6. $cPLA_2\varepsilon$ is required for recycling of cargo proteins trafficking through the clathrin-independent endocytic pathway.** (A) HeLa cells were transfected with Myc-tagged $cPLA_2\varepsilon$, fixed and stained with antibodies against CD55, CD147 or CD98. Immunofluorescence analysis revealed substantial $cPLA_2\varepsilon$ colocalization with CD55, CD147 and CD98 both at the level of vesicular structures (arrowheads) and tubular element (arrows). (B,C) Control and $cPLA_2\varepsilon$-silenced cells were incubated with antibody against CD55 at 4˚C to allow it to bind to the cell surface. Then the cells were washed and shifted to 37˚C for 30 minutes in the presence of cytochalasin D to synchronize internalized CD55 antibody in the recycling compartment. The cells were then fixed directly or incubated for an additional 30 minutes with cytochalasin-D-free medium to allow CD55 recycling to the cell surface. Before fixation the cells were subjected to acid wash to eliminate CD55 signal from the cell surface. The cells were further permeabilized and incubated with fluorescent secondary antibody to reveal an intracellular pool of the CD55. $cPLA_2\varepsilon$ silencing did not significantly affect the CD55 uptake (top row) but induced retention of CD55 upon activation of the recycling (bottom row). Quantification of normalized fluorescence (means ± s.d., $n=30$ cells) was performed as shown in Fig. 5H and revealed a significantly higher amount of CD55 retained in $cPLA_2\varepsilon$-silenced cells 30 minutes after activation of the recycling. (D) Similar recycling experiments were performed with CD147 and revealed a higher retention of internalized CD147 in $cPLA_2\varepsilon$-deficient cells despite activation of the recycling. ** $P<0.01$, *** $P<0.001$, Student's *t*-test. Scale bars: 4.2 μm (A), 8 μm (B).

expressed in HeLa cells and its intracellular distribution was investigated using confocal microscopy and compared with the wild-type enzyme. Cells expressing wild-type $cPLA_2\varepsilon$ exhibited multiple membrane tubular elements (Fig. 7D). In contrast, such tubular structures were significantly reduced in $cPLA_2\varepsilon^{S420A}$-positive cells (Fig. 7D,E) and the mutant enzyme was detected along the plasma membrane as well as at the number of the endosome-like intracellular membrane compartments (Fig. 7D). Thus, the $cPLA_2\varepsilon^{S420A}$ isoform is capable of binding to the membranes (similar to the wild-type protein), but does not support tubule formation owing to the loss of catalytic activity.

Next, we checked to what extent targeting of $cPLA_2\varepsilon^{S420A}$ to the clathrin-independent endocytic/recycling pathway was preserved. Confocal microscopy revealed that, similar to $cPLA_2\varepsilon$, the mutant enzyme was found in endocytic structures containing internalized MHC-I (Fig. 7F,G arrowheads), a main cargo marker of the clathrin-independent pathway. Therefore, targeting of the $cPLA_2\varepsilon$ to the clathrin-independent compartments appeared to be unaffected by the S420A mutation. However, in contrast to $cPLA_2\varepsilon$-positive cells, where MHC-I tubular elements were detected (Fig. 7F, arrows), the pattern of MHC-I localization was altered upon $cPLA_2\varepsilon^{S420A}$ expression. Cells that expressed $cPLA_2\varepsilon^{S420A}$ exhibited a significant reduction of MHC-I tubules (Fig. 7G), indicating that activity of the enzyme is needed for their formation.

Journal of Cell Science (2014) 127, 977–993 doi:10.1242/jcs.136598

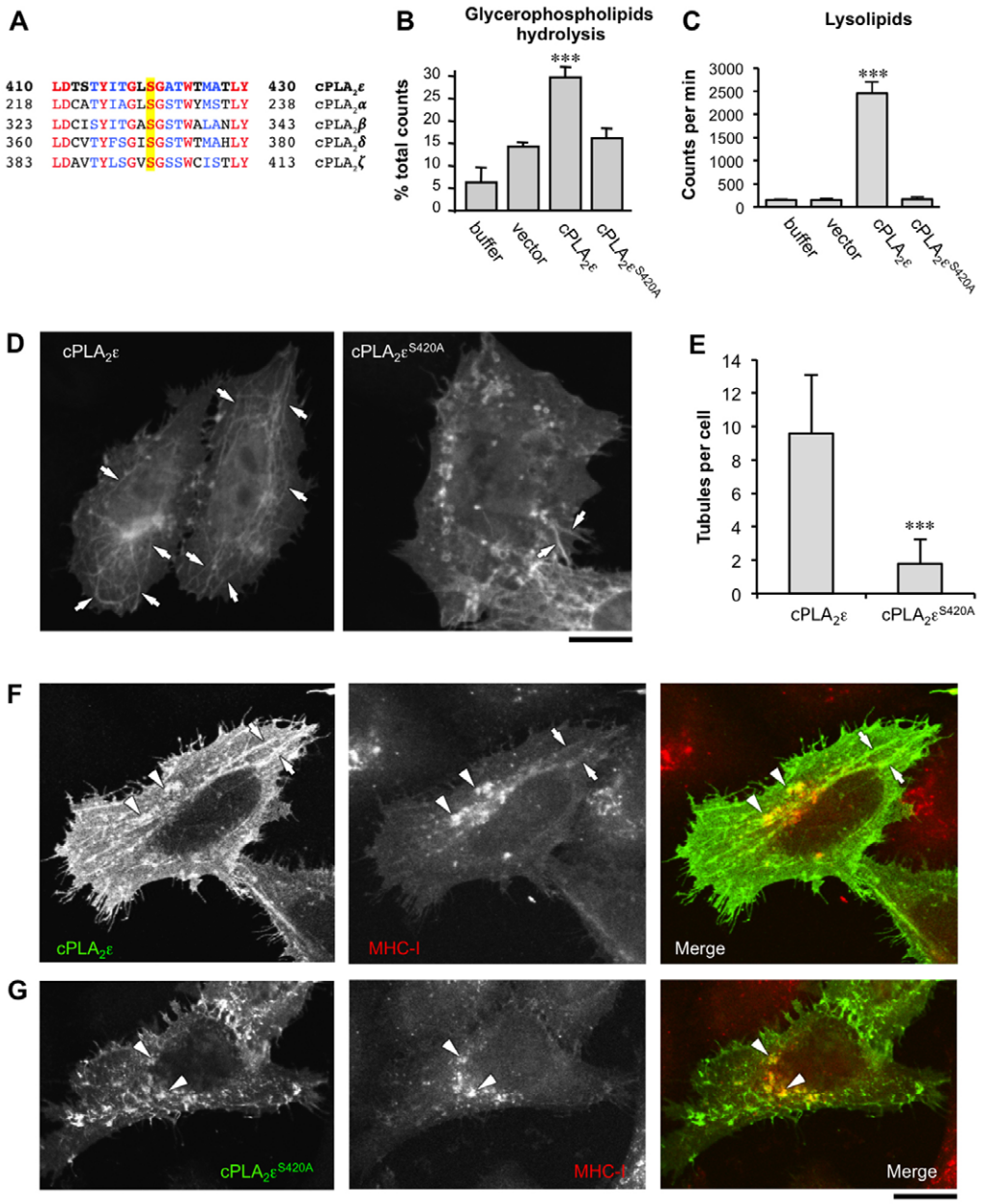


**Fig. 7. Catalytically inactive cPLA$_2$ε$^{S420A}$ mutant does not support formation of MHC-I membrane tubules.** (A) Alignment of group IV PLA2 family of enzymes catalytic domain was performed using UniProt Blast tool (identity is shown in red and similarity in blue) and revealed key serine 420 residue (highlighted in yellow) of the active site conserved among those isoforms. On the basis of the studies of sequence similarities, a cPLA$_2$ε$^{S420A}$ point mutant was generated. (B) HEK293T cells were transfected with empty pCMV–Myc vector or vectors encoding Myc–cPLA$_2$ε and Myc–cPLA$_2$ε$^{S420A}$. Then glycerophospholipid hydrolysis (quantified as percentage of total counts; means ± s.d., $n$=4 experiments) was evaluated. The cells expressing cPLA$_2$ε exhibit a significant increase in phospholipase activity, whereas transfection of cPLA$_2$ε$^{S420A}$ did not result in any increase in glycerophospholipid hydrolysis. (C) HEK293T cells were transfected with empty pCMV–Myc vector or cDNAs encoding either Myc–cPLA$_2$ε or Myc–cPLA$_2$ε$^{S420A}$. Then lysolipid production (means ± s.d., $n$=4 experiments) was evaluated. Lysolipids were detected to increase significantly in cells expressing cPLA$_2$ε, whereas cPLA$_2$ε$^{S420A}$ transfection did not enhance lysolipid generation. (D,E) HeLa cells were transfected with either Myc–cPLA$_2$ε or Myc–cPLA$_2$ε$^{S420A}$, fixed and stained with antibodies against Myc. Confocal microscopy revealed cPLA$_2$ε to induce formation of numerous tubular elements (D, left panel, arrows), whereas only few tubular elements were detected in the cells expressing cPLA$_2$ε$^{S420A}$ (D, right panel, arrows). The number of tubules (means ± s.d., $n$=50 cells) was significantly reduced in cells expressing cPLA$_2$ε$^{S420A}$ (E) (F,G) HeLa cells were transfected with Myc-tagged cPLA$_2$ε or cPLA$_2$ε$^{S420A}$ and then incubated for 30 minutes at 4°C with anti-MHC-I antibody to label MHC-I at the cell surface. After incubation, cells were washed and incubated at 37°C for 30 minutes to fill the entire clathrin-independent endocytic route. After brief acid washing to remove surface-bound antibody, cells were fixed, permeabilized and labeled with an Alexa Fluor 488 secondary antibody to reveal internalized MHC-I and with anti-Myc antibody to reveal cPLA$_2$ε or cPLA$_2$ε$^{S420A}$. Confocal images show that both cPLA$_2$ε and cPLA$_2$ε$^{S420A}$ are associated with MHC-I-positive vacuolar endosomes (F,G; arrowheads), whereas MHC-I tubular structures containing the enzyme were detected only in cells expressing cPLA$_2$ε (F; arrows). ***$P$<0.001, Student's $t$-test. Scale bars: 4.2 μm (D,F,G).

To confirm the requirement of cPLA$_2$ε activity for recycling through the clathrin-independent pathway, we investigated whether cPLA$_2$ε$^{S420A}$ is capable of rescuing the delay of the MHC-I retrieval to the cell surface in cPLA$_2$ε-silenced cells. To this end, cPLA$_2$ε-depleted cells were transfected with either cPLA$_2$ε or cPLA$_2$ε$^{S420A}$, loaded with an anti-MHC-I antibody,

Journal of Cell Science (2014) 127, 977–993 doi:10.1242/jcs.136598

and subjected to cytochalasin D block to prompt accumulation of MHC-I in the clathrin-independent endocytic compartment. Then, the cytochalasin D block was released to investigate the fate of intracellular MHC-I. Analysis of the silenced cells 30 minutes after cytochalasin D wash-out, revealed a significant amount of MHC-I that was still retained within the perinuclear compartment (Fig. 8A,B), whereas cPLA$_2$ε overexpression reduced the intracellular pool of the MHC-I (Fig. 8C,D) by reactivation of the recycling. Unlike the wild-type enzyme, cPLA$_2$ε$^{S420A}$ was unable to rescue MHC-I transport, because the amount of MHC-I in cells that expressed the inactive mutant enzyme was similar to that of the untransfected silenced cells (Fig. 8E–G). Thus, taken together, the above results suggest that the catalytic activity of cPLA$_2$ε is required to drive the formation of clathrin-independent tubular elements and to support recycling through the MHC-I route.

## DISCUSSION

Membrane trafficking, and in particular events associated with generation of transport carriers, cause local changes in the

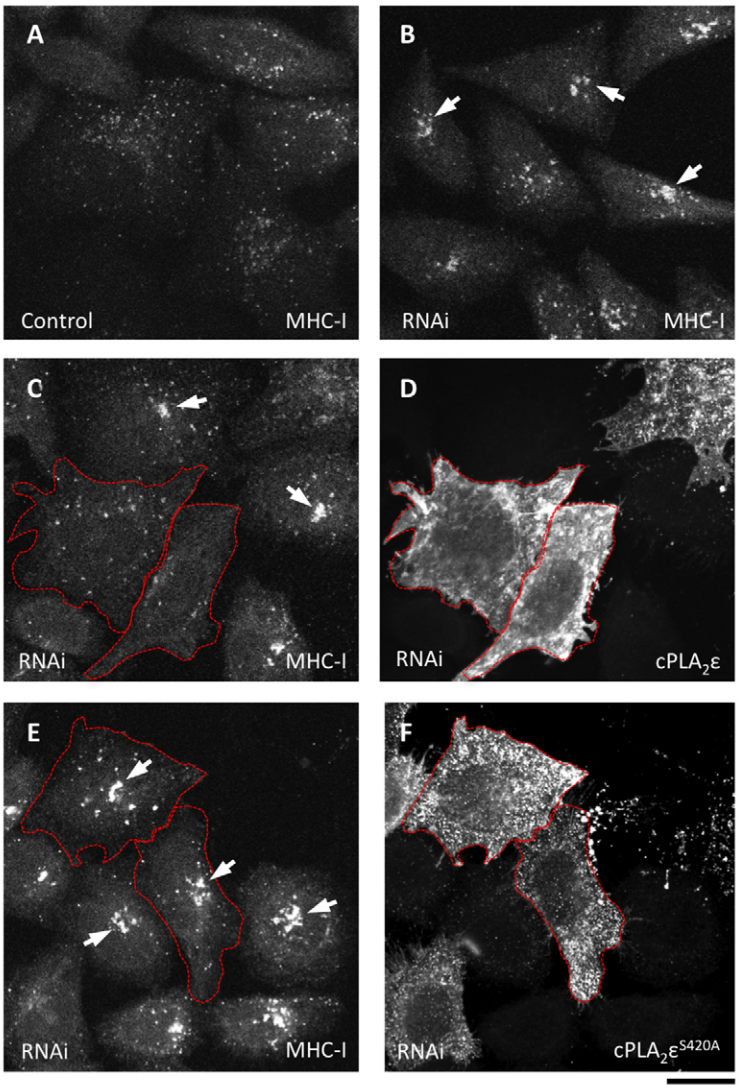


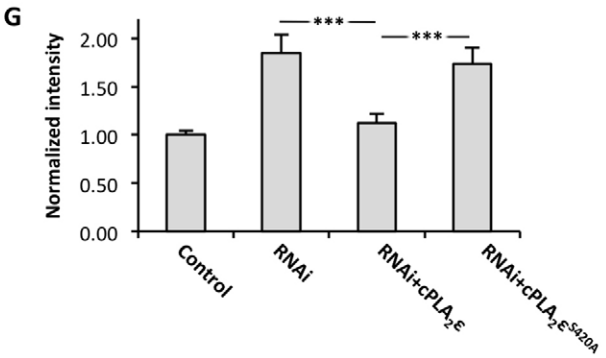


**Fig. 8. Catalytic activity of cPLA$_2$ε is required to support MHC-I recycling.** (A–F) HeLa cells were treated with scramble (A) and cPLA$_2$ε-specific siRNA (B) for 96 hours. Two additional sets of siRNA-treated cells were also transfected with mouse Myc–cPLA$_2$ε (C,D) or with its inactive mutant cPLA$_2$ε$^{S420A}$ (E,F). At the end of the siRNA treatment the cells were incubated for 30 minutes at 4°C with an anti MHC-I antibody to label MHC-I present at the cell surface (binding step). After incubation, the cells were washed and kept in cytochalasin D containing medium at 37°C for 30 minutes to allow internalization of MHC-I and to prevent its recycling back to the cell surface. Then the cells were subjected to acid wash to remove the antibody still present at the plasma membrane and incubated in cytochalasin D for 30 minutes to activate recycling. Before fixation, the cells were subjected to acid wash and remaining intracellular MHC-I was revealed using secondary fluorescent antibody. Control cells exhibited low levels of internalized MHC-I (A), whereas cPLA$_2$ε-silenced cells revealed accumulation of endocytosed MHC-I in the perinuclear recycling compartment (B; arrows). Such accumulation of MHC-I (C,D; arrows) in cPLA$_2$ε-deficient cells was in contrast to overexpression of cPLA$_2$ε (C,D; cells outlined by dashed line). cPLA$_2$ε$^{S420A}$ overexpression (E,F; cells outlined by dash line) failed to rescue internalized MHC-I from retention in the perinuclear compartment (E,F; arrows). (G) Fluorescence signal associated with internalized MHC-I was quantified in the cells treated as described above and was normalized to MHC-I fluorescence in control cells. The graph shows that normalized MHC-I fluorescence (means ± s.d., $n$=30 cells) increases upon cPLA$_2$ε RNAi. cPLA$_2$ε overexpression reduced MHC-I signal in cPLA$_2$ε-silenced cells, whereas cPLA$_2$ε$^{S420A}$ mutant did not impact MHC-I increase induced by cPLA$_2$ε ablation. ***$P$<0.001, Student's $t$-test. Scale bar: 7 μm (A–F).

Journal of Cell Science (2014) 127, 977–993 doi:10.1242/jcs.136598

physical properties of membrane bilayers that, in turn, are usually associated with variation in the composition of both lipids and protein. To execute this process, cells host a vast repertoire of mechanisms to allow dynamic and reversible membrane remodeling associated with transport carrier biogenesis through activity of membrane-associated proteins and lipid-modifying enzymes (Graham and Kozlov, 2010; McMahon and Gallop, 2005). Among the latter, $PLA_2$ enzymes have emerged as important regulators of transport processes, which rely on biogenesis of membrane tubular structures (Bechler et al., 2012; Ha et al., 2012; Polishchuk et al., 2009).

We now provide evidence for the role of a recently identified cPLA$_2$ε in trafficking through the clathrin-independent endocytic route. We found that cPLA$_2$ε is specifically associated with the clathrin-independent endocytic pathway, where it regulates the recycling process through the formation of tubular elements that carry internalized clathrin-independent cargoes back to the cell surface (Fig. 9A).

### Polybasic C-terminal stretch is a new targeting motif for compartmentalization of cytosolic $PLA_2$

Our findings are similar to those of recent studies that demonstrated a nearly identical involvement of other $PLA_2$ enzymes in membrane tabulation, which is needed for intra-Golgi transport (San Pietro et al., 2009), protein export from the TGN (Bechler et al., 2010) and recycling of endocytosed transferrin (Bechler et al., 2011). The notion that distinct $PLA_2$ enzymes were found to support non-overlapping trafficking steps suggests that each $PLA_2$ isoform possesses an array of targeting signals for specific compartmentalization. This, in turn, allows any given $PLA_2$ enzyme to generate tubular transport carriers in a specific segment of either the secretory or endocytic route. How do such signals operate to ensure correct compartmentalization of the $PLA_2$ enzymes?

Among the members of cPLA$_2$ family, the N-terminal C2 domain is considered to be the main targeting determinant that, upon increase in cytosolic $Ca^{2+}$ concentrations, promotes the enzyme binding to the correct membrane domain (Ghosh et al., 2006b). In contrast to other cPLA$_2$ enzymes, binding of cPLA$_2$ε to clathrin-independent endocytic membranes requires neither $Ca^{2+}$ nor the C2 domain and relies on a KKRxR polybasic (PB) stretch at the C-terminus, which is capable of interacting with PI(4,5)$P_2$ (Heo et al., 2006). We propose that this novel mechanism of $Ca^{2+}$-independent targeting allows cPLA$_2$ε to be compartmentalized differently than the other cPLA$_2$ enzymes. Among the other members of the cPLA$_2$ group, only cPLA$_2$β contains a similar PB sequence at its C-terminus. However, it is not clear to what extent the PB domain contributes to localization of cPLA$_2$β because the involvement of the C2 domain in cPLA$_2$β membrane binding was clearly documented (Ghosh et al., 2006b). cPLA$_2$α lacks the C-terminal PB domain and is normally targeted to the Golgi and ER membranes when cytosolic $Ca^{2+}$ increases (Evans et al., 2001). Recently, a cluster of positively charged amino acids in the central part of the cPLA$_2$α catalytic domain has been reported to determine enzyme targeting to the phagosome cup in macrophages (Casas et al., 2010). The presence of this positively-charged cluster might also explain why some cPLA$_2$α can be detected at CD59-positive endosomes (Cai et al., 2012) involved in the clathrin-independent endocytic pathway and contain elevated amounts of PI(4,5)$P_2$ similar to phagosomes (Botelho et al., 2000). These findings, however, are in contrast with recent data on the ability of the cPLA$_2$α C2 domain to bind to the phagosome alone (Zizza et al., 2012). Moreover, others have demonstrated that the PB domain operates

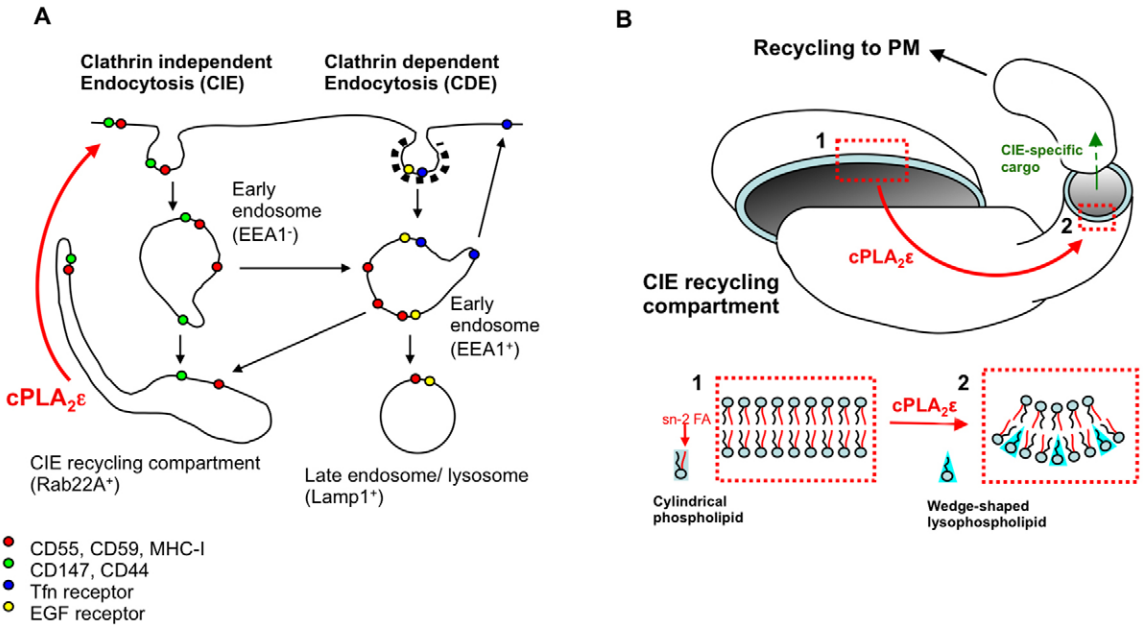


**Fig. 9. Schematic illustration of cPLA$_2$ε action in the clathrin-independent endocytic/recycling pathway.** (A) The scheme illustrates trafficking of clathrin-independent (red and green circles) and clathrin-dependent (blue and yellow circles) cargo proteins through the endocytic system. cPLA$_2$ε drives formation of tubular elements at the level of clathrin-independent recycling compartments and therefore supports recycling of clathrin-independent cargo proteins back to the cell surface (red arrow). (B) Inset 1, cPLA$_2$ε hydrolyses the fatty acids (FA) at the *sn-2* position of cylindrical phospholipids to form wedge-shaped lysophospholipids. Inset 2, this formation of wedge-shaped lysophospholipids favors generation of spontaneous membrane curvature and transformation of endosome membrane with relatively low curvature into highly curved tubular membranes, which operate in the recycling of clathrin-independent cargoes towards the plasma membrane.

Journal of Cell Science (2014) 127, 977–993 doi:10.1242/jcs.136598

in the regulation of cPLA$_2$α catalytic activity rather than in enzyme targeting (Tucker et al., 2009). This indicates that cPLA$_2$ε is the only member of the family that heavily relies on the C-terminal basic patch to be targeted to the appropriate intracellular compartment.

#### Role of phosphoinositide lipids in targeting of cPLA$_2$ε

We found that the C-terminal portion of cPLA$_2$ε, which contains the PB domain as well as the full-length enzyme, binds *in vitro* to a number of phosphoinositides, as is expected for proteins with the PB cluster (Heo et al., 2006). Several lines of evidence, however, suggest that *in vivo*, cPLA$_2$ε exhibits a higher affinity for PI(4,5)P$_2$-enriched membranes. First, cPLA$_2$ε was found to overlap with the PI(4,5)P$_2$ marker PH-PLCδ along tubular and vacuolar structures of the clathrin-independent endocytic route. Second, a strong overexpression of PH-PLCδ resulted in displacement of cPLA$_2$ε from the clathrin-independent endocytic membranes, probably because of competition for the same PI(4,5)P$_2$ binding sites (Fig. 4C). Third, we observed significant dissociation of cPLA$_2$ε from the membranes upon treatment with ionomycin, which stimulated PI(4,5)P$_2$ hydrolysis by PLC (Heo et al., 2006). Finally, we found that cPLA$_2$ε was strongly recruited to PI(4,5)P$_2$-enriched vacuoles that form in HeLa cells upon overexpression of ARF$^{Q67L}$ (Naslavsky et al., 2003). Notably, the ability of cPLA$_2$ε to bind to such vacuoles was lost after truncation of the PB motif.

Among the other PI-specific probes, only SARA-FYVE exhibits some overlap with cPLA$_2$ε at the intracellular endocytic structures, indicating that the enzyme also interacts with PI(3)P-enriched membranes. This probably allows cPLA$_2$ε to escort incoming clathrin-independent endosomes even when the PI(4,5)P$_2$ to PI(3)P switch happens in their membranes as a result of the intersection with the conventional clathrin-dependent endocytic route (Naslavsky et al., 2003).

Further along the clathrin-independent pathway, cPLA$_2$ε continues to remain associated with recycling tubular elements, where, as reported, PI(3)P is exchanged back to PI(4,5)P$_2$ and the clathrin-independent cargoes are sorted from other endocytosed molecules (Naslavsky et al., 2003). Therefore, specific PI-binding properties support targeting of cPLA$_2$ε to the compartments of the clathrin-independent route. Furthermore, PIPs have been shown to promote cPLA$_2$ε activity (Ghomashchi et al., 2010) indicating that a specific PIP composition is likely to be required, not only for targeting but also for the activity of the enzyme.

Interestingly, the specific binding of the other PLA$_2$ enzyme PAFAH-Ib to PI(4)P and PI(3)P was convincingly documented and hypothesized to play a key role in the association of PAFAH-Ib with Golgi and early endosome membranes, respectively (Bechler et al., 2011). In contrast to cPLA$_2$ε, the precise PIP-binding portion of PAFAH-Ib remains to be identified (Bechler et al., 2011). Nonetheless, the example of cPLA$_2$ε and PAFAH-Ib reveals the affinity for specific PIP(s) as a novel and important mechanism that contributes to differential compartmentalization of the PLA$_2$ enzymes.

#### cPLA$_2$ε specifically functions in the clathrin-independent endocytic/recycling pathway

Taking into consideration the selective association of cPLA$_2$ε with clathrin-independent endocytic membranes, we expected the enzyme to operate in the transport processes that occur within this route. Although the protein is distributed along both incoming and recycling membranes of the clathrin-independent pathway, we found that cPLA$_2$ε is required only for a subset of transport events along the clathrin-independent pathway. Depletion of cPLA$_2$ε affects neither uptake of clathrin-independent-specific cargo MHC-I nor its subsequent delivery to the perinuclear recycling compartment. However, further trafficking of MHC-I was impaired in cPLA$_2$ε-depleted cells because of a significant reduction in the tubular elements involved in MHC-I recycling back to the plasma membrane. Therefore, cPLA$_2$ε is required specifically for tubule-mediated transport events. In contrast, the cPLA$_2$ε apparently does not operate in the uptake and early clathrin-independent endocytic trafficking steps, where the generation of tubular membranes has not been reported (Donaldson et al., 2009; Grant and Donaldson, 2009).

Surprisingly, cPLA$_2$α was recently detected at CD59-positive endosomes where the enzyme interacts with EHD1 and induces fission and vesiculation of CD59-positive tubular elements (Cai et al., 2012). At first glance these findings appear to be in contrast with the expected role of cytosolic PLA$_2$ enzymes to support membrane tubulation (Bechler et al., 2011; Bechler et al., 2010; San Pietro et al., 2009; Yang et al., 2011). However, the function of cPLA$_2$α in clathrin-independent endocytosis might require a complex interplay with EHD1 (Cai et al., 2012). Moreover, in contrast to cPLA$_2$ε, suppression of cPLA$_2$α seems to have very mild impact on trafficking through the clathrin-independent endocytic route (Cai et al., 2012). Therefore, a specific contribution of each of the above cPLA$_2$ enzymes in membrane morphogenesis and trafficking along the clathrin-independent pathway should be carefully examined in future.

Notably, the inhibitory impact of cPLA$_2$ε depletion was specific for the clathrin-independent route. Other endocytic/recycling pathways remained almost perfectly functional in cPLA$_2$ε-deficient cells despite a number of those pathways being operated through tubular elements. For instance, tubule-mediated processes such as sorting of M6PR from the endosomes to the TGN (Bonifacino and Rojas, 2006; Cullen, 2008) or recycling of internalized Tfn to the plasma membrane (Bonifacino and Rojas, 2006; Cullen, 2008) were not seriously challenged by knockdown of cPLA$_2$ε. This is probably due to the relatively poor association of cPLA$_2$ε with the membranes involved in Tfn and M6PR trafficking (see Fig. 1). Thus, other PLA$_2$ enzymes (or even different molecular mechanisms) are likely to drive the formation of tubular elements in M6PR and Tfn recycling pathways. Indeed, the biogenesis of the tubular membranes that recycle Tfn back to the cell surface has been shown to require the PLA$_2$ activity of PAFAH-Ib (Bechler et al., 2011). Meanwhile, whether the biogenesis of M6PR tubules from the endosomes involves any PLA$_2$ enzyme is yet to be determined.

#### Catalytic activity of cPLA$_2$ε is required for tubule formation and recycling through the clathrin-independent route

The selectivity of cPLA$_2$ε for the clathrin-independent pathway prompted us to investigate the mechanism through which the enzyme regulates biogenesis of the tubular elements involved in recycling of clathrin-independent cargoes. The elucidation of this mechanism is of great importance given that the proteins that use this transport pathway play a significant role in a number of physiological and pathological processes, such as immune surveillance and defense (MHC-I, CD55, CD59) (Ferrone et al., 2000; Gelderman et al., 2004), cell adhesion (β1-integrin) (Brown et al., 2001) and tumor cell invasion (CD147 and CD98) (Cantor and Ginsberg, 2012; Guo et al., 2000). This makes cPLA$_2$ε an

Journal of Cell Science (2014) 127, 977–993 doi:10.1242/jcs.136598

appealing target for the development of specific chemical inhibitors or activators that would regulate surface exposure and hence also regulate the specific activities of the clathrin-independent proteins.

We found that the catalytic activity of cPLA$_2$ε is required to support formation of the membrane tubules that mediate clathrin-independent recycling, because it has also been reported for other PLA$_2$ enzymes (Bechler et al., 2011; Bechler et al., 2010; San Pietro et al., 2009; Yang et al., 2011). Although a specific cPLA$_2$ε inhibitor is still not available, we used an inactive cPLA$_2$ε$^{S420A}$ mutant to confirm this. This mutant is capable of binding to the clathrin-independent endocytic compartments, but lacks the capacity to hydrolyze phospholipids into lysolipids. As a consequence, expression of cPLA$_2$ε$^{S420A}$ did not induce clathrin-independent tubule growth and, therefore, failed to rescue MHC-I recycling in cPLA$_2$ε-depleted cells. In contrast, overexpression of fully functional cPLA$_2$ε triggered massive tubulation of clathrin-independent endocytic membranes that carry MHC-I (see Fig. 7), probably because of the strong increase in lysolipid production.

These findings indicate that cPLA$_2$ε is a missing piece of the molecular puzzle that operates in membrane-remodeling events associated with recycling in the clathrin-independent route. Indeed, the core components of this puzzle have already been uncovered. This process apparently requires ARF6-dependent activation of PI(4)P5-kinase (Donaldson et al., 2009). PI(4)P5-kinase produces PI(4,5)P$_2$, which allows binding of cPLA$_2$ε to clathrin-independent endosomes, where the enzyme supports biogenesis of tubular membranes through the generation of wedge-shaped lysolipids (Fig. 9B). However, PI(4,5)P$_2$ provides an attractive binding site for PLD2 (Donaldson, 2009), which produces negatively-curved phosphatidic acid (Donaldson et al., 2009; Yang et al., 2008; Zimmerberg and Kozlov, 2006) and, therefore, favors fission of the clathrin-independent endocytic tubular elements into recycling transport carriers (Donaldson, 2009). Thus, the interplay between cPLA$_2$ε and PLD2 activities is likely to play a key role in the regulation of transport carrier biogenesis in the clathrin-independent route. Interestingly, similar roles in tubular biogenesis and fission were demonstrated for cPLA$_2$α and PLD2 enzymes at the Golgi membranes (San Pietro et al., 2009; Yang et al., 2008; Yang et al., 2011). Thus, it will be important to identify the proteins that interact with cPLA$_2$ε to control its activity and to understand how such proteins are integrated in the molecular signaling network that drives transport events within the clathrin-independent endocytic/recycling route.

## MATERIALS AND METHODS

### Recombinant DNA constructs and cDNA mutagenesis

DNA was from the following sources: GFP–cPLA$_2$ε from T. Shimizu (University of Tokyo, Japan), GFP–Rab22a from R. Weigert (NIH, USA), Myc–EHD1 from S. Caplan (University of Nebraska, USA), ARF6 from J. Donaldson (NIH, USA) and GFP–cPLA$_2$α C. Leslie (NJMRC, USA), GFP-tagged PH-PLCδ, CERT-PH, GRP1-PH and SARA-FIVE was from M. A. De Matteis (TIGEM, Italy). The mouse cPLA$_2$ε was then subcloned from pEGFP-C1 into different N-terminal tagged vectors. It was first amplified by PCR using the following primers: CGGAATTCAAATGCAGTCTATTCCACACT (forward) and ACCTCGAGACTAGGAGGGACACTGGCTCCT (reverse), and cloned into *Eco*RI and *Xho*I sites of the p-Myc–CMV vector (Clontech, Mountain View, CA), p*m*-Cherry-CMV vector (provided by G. Burgstaller) and pGEX4T.1 (GE Healthcare Life Sciences). Human cPLA$_2$ε N-tail (amino acids 1–63) was PCR amplified from PLA2G4E human DNA using primers: CG GAA TTC ATG CGC GCC AAG TGC ATT AC (forward) and CCG CTC GAG AGG AAC CTG CTC AGC CCT C (reverse), and cloned into *Eco*RI and *Xho*I sites of the pGEX4T.1. The pGEX4T.1- cPLA$_2$ε C-tail (amino acids 815–875) was PCR amplified from mouse pEGFP-cPLA$_2$ε using primers: CG AGA TCT CTG GGC CAG CTG AAC ATC T (forward) and CG GAA TTC CTA GGA GGG ACA CTG GCT (reverse), and cloned into *Bgl*II and *Eco*RI sites of pGEX4T.1. Myc–cPLA$_2$ε$^{S420A}$ and Myc–cPLA$_2$εΔPB were prepared by site-directed mutagenesis with the QuikChange kit (Stratagene, La Jolla, CA). For the Myc–cPLA2εS420A mutant, the forward and reverse primer sequences were: ACA TCA CCG GCT TGG CAG GTG CAA CCT GG (forward) and CCA GGT TGC ACC TGC CAA GCC GGT GAT GT (reverse). Myc–cPLA$_2$εΔPB was obtained by introducing a stop codon at position 865. The forward and reverse primers were: TTG AGA CTA GCA ATG ***T***AG AAG AAA CGC ATG A (forward) and T CAT GCG TTT CTT CTA CAT TGC TAG TCT CAA (reverse).

### RNA interference

Oligonucleotide duplexes (5′-GGG UCA UGG CUG UCC AAU U-3′ and 5′-AAU UGG ACA GCC AUG ACC C-3′) targeting human cPLA$_2$ε were from Qiagen. siCONTROL, a universal negative control siRNA, was from Sigma. SiRNA delivery into HeLa cells was executed using Lipofectamine 2000 (Invitrogen, Carlsbad, CA). Cells were incubated with siRNA for 96 hours to achieve optimal cPLA$_2$ε suppression (evaluated by immunoblot analysis). Quantification of western blots was performed using the ECL western blotting system (Amersham Pharmacia Biotech, Little Chalfont, UK).

### Cells, reagents and antibodies

HeLa cells were grown in DMEM containing 10% FCS. Cytochalasin D, latrunculin A, BAPTA-AM, and saponin were from Sigma-Aldrich. Antibodies were obtained from the following sources: anti-MHC-I, anti-CD147, anti-CD55 and anti-CD98 from Biolegend (San Diego, CA), anti-EEA1 from Novus Biologicals (Littleton, CO), anti-c-Myc and anti-transferrin receptor from Sigma-Aldrich (St. Louis, MO), anti-Lamp1, anti-giantin and anti-GST from M. A. De Matteis (TIGEM, Naples, Italy), anti-M6PR from Chemicon (Temecula, CA), anti-HA from Covance (Princeton, NJ), anti-caveolin-1, anti-golgin-97 and anti-ARF6 from Santa Cruz Biotechnology (Dallas, TX), anti-Rabbit IgG-HRP and anti-Mouse IgG-HRP from Bethyl Laboratories (Montgomery, TX), secondary antibodies conjugated with Alexa Fluor 488 or Alexa Fluor 568, transferrin–Alexa-Fluor-568 and Alexa-Fluor-488–EGF were from Invitrogen (Carlsbad, CA). Generation of anti-cPLA$_2$ε N-tail antibody was performed according standard protocols in the protein service facility.

### Protein–lipid binding assay

PIP strips (Echelon Biosciences, Salt Lake City, UT) were blocked in TBST supplemented with 3% fatty-acid-free BSA and then incubated with 500 ng/ml of three different GST-fused cPLA$_2$ε proteins: full-length cPLA$_2$ε, N-tail cPLA$_2$ε, C-tail cPLA$_2$ε. GST-fused PH-PLCδ, p40-PX and SidC were used as positive control probes for PI(4,5)P2, PI3P and PI4P respectively, whereas GST alone was used as a negative control. At the end of the incubation, the PIP strips were washed with TBST, incubated with anti-GST antibody and revealed with an anti-mouse HRP conjugate (Amersham, Piscataway, NJ). After final washing, a chemiluminescence system (GE Healthcare, Oslo, Norway) was used to detect binding of the GST fusions to the phospholipids.

### Immunofluorescence and antibody internalization

For immunofluorescence analyses, the cells were prepared and examined with a Zeiss LSM-710 confocal microscope (Carl Zeiss, Gottingen, Germany) as described previously (Polishchuk et al., 2003). To assess internalization of the MHC-I antibody, cells were incubated with 1 µg/ml antibody against human MHC-I on ice and washed with PBS to remove the unbound antibody. At this point, a set of coverslips were fixed and incubated with secondary antibody to label the surface pool of MHC-I. The remaining cells were incubated in pre-warmed medium for varying

times to activate endocytosis of the antibody. After internalization, the cells were washed with cold PBS, the surface-bound MHC-I antibody was removed by acid wash. Finally, the cells were fixed and internalized MHC-I was revealed after using Alexa-Fluor-488- or Alexa-Fluor-546-conjugated secondary antibodies.

To perform recycling assays, an initial binding step was performed as described above. The cells were further incubated at 37℃ in the presence of 10 µM cytochalasin D to allow internalization of the surface-bound MHC-I antibody and accumulation in the recycling compartment (Weigert, 2004). The antibody that still remained bound to the cell surface was removed by acid wash. At this point, a set of coverslips were fixed, permeabilized and incubated with a secondary antibody to label the internalized anti-MHC-I IgG. Another set of coverslips was washed in PBS and then incubated at 37℃ for 30 minutes with complete medium to allow recycling of MHC-I. After this period, the treated cells were incubated with a low-pH buffer to remove the surface pool of antibody, then were fixed, permeabilized and incubated with the secondary fluorescent antibody to reveal the intracellular pool of MHC-I. CD55, CD98 and CD147 recycling assays were performed as described for MHC-I, using a 15 µg/ml concentration of the corresponding antibody.

In experiments where the internalization of Alexa-Fluor-546–transferrin (25 µg/ml) or Alexa-Fluor-488–EGF (100 ng/ml) was monitored, the cells were first incubated for 30 minutes in DMEM without serum and then were further kept at 37℃ for varying times. Cells were then washed with cold PBS to remove the unbound transferrin and incubated at 37℃ for varying times to allow internalization of Alexa-Fluor-546–Tfn. After internalization, the cells were washed with cold PBS (for Alexa-Fluor-546–Tfn, the surface-bound transferrin was removed by acid wash) and fixed.

### Image analysis

Overlap of cPLA$_2$ε with different markers of endocytic and secretory compartments was evaluated in confocal images using the colocalization module of LSM3.2 software. ROI function was used to analyze colocalization selectively in either tubular or vacuolar structures containing cPLA$_2$ε. The amount of MHC-I, CD55, CD147 or transferrin at the surface or inside the cell was estimated as follows: 30–50 cells/coverslip were randomly selected, imaged with the pinhole completely open and with identical acquisition parameters. Under these conditions, the amount of internalized cargo was proportional to the average fluorescence. For each channel, the average fluorescence of each individual cell was measured using Zeiss LSM 3.2 software.

### Phospholipase activity

HEK293T cells, transfected with pCMV-Myc vector or vectors encoding Myc–cPLA$_2$ε, Myc– cPLA$_2$ε$^{S420A}$ were disrupted by sonication in a homogenizing buffer. Centrifugation at 10,000 ***g*** for 10 minutes and 100,000 ***g*** for 1 hour were carried out for fractionation, as reported previously (Ohto, 2005). The phospholipase reaction was started by the addition of enzyme sources (400 µg of supernatant from the 100,000 ***g*** centrifugation) to substrates [30,000 cpm/sample of [$^3$H]-glycerol-labeled total cellular lipids, prepared as reported previously (Berrie et al., 2007)] in 100 mM HEPES-NaOH, pH 7.5, 1 mg/ml BSA, 4.5 mM $CaCl_2$ and 1 mM dithiothreitol, and the reaction mixture was incubated at 37℃ for 2 hours and 30 minutes. The assay was terminated by Bligh and Dyer extraction and the radioactivity recovered in the upper phase containing deacylated lipids was evaluated by liquid scintillation. The lower organic phase was dried and separated by thin layer chromatography (TLC) and the radioactivity associated with the labeled lysolipids was quantified by gas ionization scanning (Radio Isotope Thin Layer Analyzer, Raytest, Germany).

### Electron microscopy

HeLa cells were transfected with Myc-tagged cPLA$_2$ε or co-transfected with cPLA$_2$ε–Myc and ARF6$^{Q67L}$–GFP. In a subset of experiments the cells expressing cPLA$_2$ε–Myc were loaded with Alexa-Fluor-488-conjugated antibodies against MHC-I for 1 hour to allow completion of the entire clathrin-independent endocytic pathway. Cryosections were prepared and labeled as described previously (Polishchuk et al., 2003) and investigated using a Tecnai G2 Spirit BioTWIN electron microscope (FEI, Einhoven, The Netherlands) equipped with a Veletta CCD camera for digital image acquisition.

### Acknowledgements

We would like to acknowledge everybody who provided us with antibodies and DNA; Graciana Diez-Roux and Ellen Abrams for critical reading of the manuscript; and TIGEM Advanced Microscopy and Imaging Core for microscopy support.

### Competing interests

The authors declare no competing interests.

### Author contributions

M.C., S.M., R.B., A.L. and R.S.P. conceived and designed experiments. M.C., S.M., A.V.E., G.P., S.I., M.S., A.D.P., C.I., M.E. and G.D.T. performed experiments; M.C., S.M., G.P., S.I., M.V.E., R.B., A.L. and R.S.P. analyzed data; M.C. and R.S.P. wrote the manuscript.

### Funding

This work was supported by the AIRC [grant number IG 10233]; and Telethon [grant number GTF08001] to R.S.P. Part of this work was supported by a fellowship to M.C. that was provided by Banca Popolare di Lanciano e Sulmona within "uno piu uno" project and by Fondazione Negri Sud onlus.

### Supplementary material

Supplementary material available online at
http://jcs.biologists.org/lookup/suppl/doi:10.1242/jcs.136598/-/DC1

### References

**Bechler, M. E., Doody, A. M., Racoosin, E., Lin, L., Lee, K. H. and Brown, W. J.** (2010). The phospholipase complex PAFAH Ib regulates the functional organization of the Golgi complex. *J. Cell Biol.* **190**, 45-53.

**Bechler, M. E., Doody, A. M., Ha, K. D., Judson, B. L., Chen, I. and Brown, W. J.** (2011). The phospholipase $A_2$ enzyme complex PAFAH Ib mediates endosomal membrane tubule formation and trafficking. *Mol. Biol. Cell* **22**, 2348-2359.

**Bechler, M. E., de Figueiredo, P. and Brown, W. J.** (2012). A PLA1-2 punch regulates the Golgi complex. *Trends Cell Biol.* **22**, 116-124.

**Berrie, C. P., Iurisci, C., Piccolo, E., Bagnati, R. and Corda, D.** (2007). Analysis of phosphoinositides and their aqueous metabolites. *Methods Enzymol.* **434**, 187-232.

**Bonifacino, J. S. and Rojas, R.** (2006). Retrograde transport from endosomes to the trans-Golgi network. *Nat. Rev. Mol. Cell Biol.* **7**, 568-579.

**Botelho, R. J., Teruel, M., Dierckman, R., Anderson, R., Wells, A., York, J. D., Meyer, T. and Grinstein, S.** (2000). Localized biphasic changes in phosphatidylinositol-4,5-bisphosphate at sites of phagocytosis. *J. Cell Biol.* **151**, 1353-1368.

**Brown, F. D., Rozelle, A. L., Yin, H. L., Balla, T. and Donaldson, J. G.** (2001). Phosphatidylinositol 4,5-bisphosphate and Arf6-regulated membrane traffic. *J. Cell Biol.* **154**, 1007-1018.

**Cai, B., Caplan, S. and Naslavsky, N.** (2012). cPLA2α and EHD1 interact and regulate the vesiculation of cholesterol-rich, GPI-anchored, protein-containing endosomes. *Mol. Biol. Cell* **23**, 1874-1888.

**Cantor, J. M. and Ginsberg, M. H.** (2012). CD98 at the crossroads of adaptive immunity and cancer. *J. Cell Sci.* **125**, 1373-1382.

**Caplan, S., Naslavsky, N., Hartnell, L. M., Lodge, R., Polishchuk, R. S., Donaldson, J. G. and Bonifacino, J. S.** (2002). A tubular EHD1-containing compartment involved in the recycling of major histocompatibility complex class I molecules to the plasma membrane. *EMBO J.* **21**, 2557-2567.

**Casas, J., Valdearcos, M., Pindado, J., Balsinde, J. and Balboa, M. A.** (2010). The cationic cluster of group IVA phospholipase A2 (Lys488/Lys541/Lys543/Lys544) is involved in translocation of the enzyme to phagosomes in human macrophages. *J. Lipid Res.* **51**, 388-399.

**Cullen, P. J.** (2008). Endosomal sorting and signalling: an emerging role for sorting nexins. *Nat. Rev. Mol. Cell Biol.* **9**, 574-582.

**de Figueiredo, P., Doody, A., Polizotto, R. S., Drecktrah, D., Wood, S., Banta, M., Strang, M. S. and Brown, W. J.** (2001). Inhibition of transferrin recycling and endosome tubulation by phospholipase A2 antagonists. *J. Biol. Chem.* **276**, 47361-47370.

**Dennis, E. A., Cao, J., Hsu, Y. H., Magrioti, V. and Kokotos, G.** (2011). Phospholipase A2 enzymes: physical structure, biological function, disease implication, chemical inhibition, and therapeutic intervention. *Chem. Rev.* **111**, 6130-6185.

**Donaldson, J. G.** (2009). Phospholipase D in endocytosis and endosomal recycling pathways. *Biochim. Biophys. Acta* **1791**, 845-849.

**Donaldson, J. G., Porat-Shliom, N. and Cohen, L. A.** (2009). Clathrin-independent endocytosis: a unique platform for cell signaling and PM remodeling. *Cell. Signal.* **21**, 1-6.

**Doody, A. M., Antosh, A. L. and Brown, W. J.** (2009). Cytoplasmic phospholipase A2 antagonists inhibit multiple endocytic membrane trafficking pathways. *Biochem. Biophys. Res. Commun.* **388**, 695-699.
**Evans, J. H., Spencer, D. M., Zweifach, A. and Leslie, C. C.** (2001). Intracellular calcium signals regulating cytosolic phospholipase A2 translocation to internal membranes. *J. Biol. Chem.* **276**, 30150-30160.
**Evans, J. H., Gerber, S. H., Murray, D. and Leslie, C. C.** (2004). The calcium binding loops of the cytosolic phospholipase A2 C2 domain specify targeting to Golgi and ER in live cells. *Mol. Biol. Cell* **15**, 371-383.
**Eyster, C. A., Higginson, J. D., Huebner, R., Porat-Shliom, N., Weigert, R., Wu, W. W., Shen, R. F. and Donaldson, J. G.** (2009). Discovery of new cargo proteins that enter cells through clathrin-independent endocytosis. *Traffic* **10**, 590-599.
**Ferrone, S., Finerty, J. F., Jaffee, E. M. and Nabel, G. J.** (2000). How much longer will tumour cells fool the immune system? *Immunol. Today* **21**, 70-72.
**Gelderman, K. A., Tomlinson, S., Ross, G. D. and Gorter, A.** (2004). Complement function in mAb-mediated cancer immunotherapy. *Trends Immunol.* **25**, 158-164.
**Ghomashchi, F., Naika, G. S., Bollinger, J. G., Aloulou, A., Lehr, M., Leslie, C. C. and Gelb, M. H.** (2010). Interfacial kinetic and binding properties of mammalian group IVB phospholipase A2 (cPLA2beta) and comparison with the other cPLA2 isoforms. *J. Biol. Chem.* **285**, 36100-36111.
**Ghosh, M., Loper, R., Gelb, M. H. and Leslie, C. C.** (2006a). Identification of the expressed form of human cytosolic phospholipase A2beta (cPLA2beta): cPLA2beta3 is a novel variant localized to mitochondria and early endosomes. *J. Biol. Chem.* **281**, 16615-16624.
**Ghosh, M., Tucker, D. E., Burchett, S. A. and Leslie, C. C.** (2006b). Properties of the Group IV phospholipase A2 family. *Prog. Lipid Res.* **45**, 487-510.
**Graham, T. R. and Kozlov, M. M.** (2010). Interplay of proteins and lipids in generating membrane curvature. *Curr. Opin. Cell Biol.* **22**, 430-436.
**Grant, B. D. and Donaldson, J. G.** (2009). Pathways and mechanisms of endocytic recycling. *Nat. Rev. Mol. Cell Biol.* **10**, 597-608.
**Guo, H., Li, R., Zucker, S. and Toole, B. P.** (2000). EMMPRIN (CD147), an inducer of matrix metalloproteinase synthesis, also binds interstitial collagenase to the tumor cell surface. *Cancer Res.* **60**, 888-891.
**Ha, K. D., Clarke, B. A. and Brown, W. J.** (2012). Regulation of the Golgi complex by phospholipid remodeling enzymes. *Biochim. Biophys. Acta* **1821**, 1078-1088.
**Heo, W. D., Inoue, T., Park, W. S., Kim, M. L., Park, B. O., Wandless, T. J. and Meyer, T.** (2006). PI(3,4,5)P3 and PI(4,5)P2 lipids target proteins with polybasic clusters to the plasma membrane. *Science* **314**, 1458-1461.
**Luini, A., Ragnini-Wilson, A., Polishchuck, R. S. and De Matteis, M. A.** (2005). Large pleiomorphic traffic intermediates in the secretory pathway. *Curr. Opin. Cell Biol.* **17**, 353-361.
**McMahon, H. T. and Gallop, J. L.** (2005). Membrane curvature and mechanisms of dynamic cell membrane remodelling. *Nature* **438**, 590-596.
**Naslavsky, N., Weigert, R. and Donaldson, J. G.** (2003). Convergence of non-clathrin- and clathrin-derived endosomes involves Arf6 inactivation and changes in phosphoinositides. *Mol. Biol. Cell* **14**, 417-431.
**Ohto, T., Uozumi, N., Hirabayashi, T. and Shimizu, T.** (2005). Identification of novel cytosolic phospholipase A(2)s, murine cPLA(2)delta, epsilon, and zeta, which form a gene cluster with cPLA(2)beta. *J. Biol. Chem.* **280**, 24576-24583.
**Polishchuk, E. V., Di Pentima, A., Luini, A. and Polishchuk, R. S.** (2003). Mechanism of constitutive export from the golgi: bulk flow via the formation, protrusion, and en bloc cleavage of large trans-golgi network tubular domains. *Mol. Biol. Cell* **14**, 4470-4485.
**Polishchuk, R. S., Capestrano, M. and Polishchuk, E. V.** (2009). Shaping tubular carriers for intracellular membrane transport. *FEBS Lett.* **583**, 3847-3856.
**Saftig, P. and Klumperman, J.** (2009). Lysosome biogenesis and lysosomal membrane proteins: trafficking meets function. *Nat. Rev. Mol. Cell Biol.* **10**, 623-635.
**San Pietro, E., Capestrano, M., Polishchuk, E. V., DiPentima, A., Trucco, A., Zizza, P., Mariggiò, S., Pulvirenti, T., Sallese, M., Tete, S. et al.** (2009). Group IV phospholipase A(2)alpha controls the formation of inter-cisternal continuities involved in intra-Golgi transport. *PLoS Biol.* **7**, e1000194.
**Schaloske, R. H. and Dennis, E. A.** (2006). The phospholipase A2 superfamily and its group numbering system. *Biochim. Biophys. Acta* **1761**, 1246-1259.
**Sprong, H., van der Sluijs, P. and van Meer, G.** (2001). How proteins move lipids and lipids move proteins. *Nat. Rev. Mol. Cell Biol.* **2**, 504-513.
**Tucker, D. E., Ghosh, M., Ghomashchi, F., Loper, R., Suram, S., John, B. S., Girotti, M., Bollinger, J. G., Gelb, M. H. and Leslie, C. C.** (2009). Role of phosphorylation and basic residues in the catalytic domain of cytosolic phospholipase A2alpha in regulating interfacial kinetics and binding and cellular function. *J. Biol. Chem.* **284**, 9596-9611.
**Weigert, R., Yeung, A. C., Li, J. and Donaldson, J. G.** (2004). Rab22a regulates the recycling of membrane proteins internalized independently of clathrin. *Mol. Biol. Cell* **15**, 3758-3770.
**Yang, J. S., Gad, H., Lee, S. Y., Mironov, A., Zhang, L., Beznoussenko, G. V., Valente, C., Turacchio, G., Bonsra, A. N., Du, G. et al.** (2008). A role for phosphatidic acid in COPI vesicle fission yields insights into Golgi maintenance. *Nat. Cell Biol.* **10**, 1146-1153.
**Yang, J. S., Valente, C., Polishchuk, R. S., Turacchio, G., Layre, E., Moody, D. B., Leslie, C. C., Gelb, M. H., Brown, W. J., Corda, D. et al.** (2011). COPI acts in both vesicular and tubular transport. *Nat. Cell Biol.* **13**, 996-1003.
**Zimmerberg, J. and Kozlov, M. M.** (2006). How proteins produce cellular membrane curvature. *Nat. Rev. Mol. Cell Biol.* **7**, 9-19.
**Zizza, P., Iurisci, C., Bonazzi, M., Cossart, P., Leslie, C. C., Corda, D. and Mariggiò, S.** (2012). Phospholipase A2IVα regulates phagocytosis independent of its enzymatic activity. *J. Biol. Chem.* **287**, 16849-16859.